Extended Wittrick-Williams algorithm for eigenvalue solution of stochastic dynamic stiffness method

Xiang Liu[a,b,c], Xiao Liu[a,b,c], Sondipon Adhikari[d], Shengwen Yin[a,b,c]

[a]Key Laboratory of Traffic Safety on Track, Ministry of Education, School of Traffic & Transportation Engineering, Central South University, Changsha, China
[b]Joint International Research Laboratory of Key Technology for Rail Traffic Safety, Central South University, Changsha, China
[c]National & Local Joint Engineering Research Center of Safety Technology for Rail Vehicle, Central South University, Changsha, China
[d]College of Engineering, Swansea University, Singleton Park, Swansea SA2 8PP, UK.

Abstract

This paper proposes an efficient and reliable eigenvalue solution technique for analytical stochastic dynamic stiffness (SDS) formulations of beam built-up structures with parametric uncertainties. The SDS formulations are developed based on frequency-dependent shape functions in conjunction with both random-variable and random-field structural parameters. The overall numerical framework is aimed towards representing the broadband dynamics of structures using very few degrees of freedom. This paper proposes a novel approach combining the Wittrick-Williams algorithm, the Newton iteration method and numerical perturbation method to extract eigensolutions from SDS formulations. First, the eigenvalues and eigenvectors of the deterministic DS formulations are computed by the WW algorithm and the corresponding mode finding technique, which are used as the initial solution. Then, a numerical perturbation technique based on the inverse iteration and homotopy method is proposed to update the eigenvectors and eigenvalues. The robustness and efficiency of the proposed method are guaranteed through several technique arrangements. Through numerical examples, the proposed method is demonstrated to be robust within the whole frequency range. This method provides an efficient and reliable tool for stochastic analysis of eigenvalue problems relevant to free vibration and buckling analysis of built-up structures.

Keywords: Stochastic eigenvalue solution; Stochastic dynamic stiffness method; Wittrick-Williams algorithm; Numerical perturbation method; Random field; Karhunen-Loève expansion.

1. Introduction

It is well-acknowledged that the dynamic properties of built-up structures are affected by the uncertainties of their physical properties, such as material properties, geometric

dimensions, boundary conditions and etc. As a result, the dynamic properties of complex built-up structures such as trains, airplanes or machines behavior in a stochastic way, which are significantly influenced by manufacturing and assembling techniques as well as the operating environment. However, uncertainties are not taken into consideration in most of structure design, instead, deterministic prediction models are used, leading to deterministic analysis and design. In this respect, the safety factor method is usually employed in engineering practice, which sometimes leads to either uneconomical or unsafe designs. In many high-end equipment manufacturing industries, it becomes more and more necessary to take parameter uncertainties into account in their modelling, guaranteeing high-fidelity design.

Modal analysis is a fundamental technique in the analysis and design of engineering systems [1–5], which is essentially an eigenvalue problem leading to either natural frequencies and natural modes or critical buckling loads and buckling modes. In real engineering practice, those engineering systems contain uncertainties in, e.g. material and geometric parameters, which no doubt lead to uncertainties into the related eigenvalues and mode shapes. For dynamical analysis, free vibration modal analysis is the first step to obtain the dynamic statistics of linear stochastic dynamic systems. Stochastic eigenvalue problems also arise in the stability analysis of linear systems with random imperfections. The study of probabilistic characterization of the eigensolutions of random matrix and differential operators is an important research topic in the field of stochastic structural mechanics since the mid-1960s [6]. For example, the stochastic eigenvalues problems could arise from both discrete systems or continuous systems[7]. The randomness of structural or geometries parameters[8] can be described by either random variable models or random field [9]. In particular, the random variable model doesn't consider the variability of structural parameters in spatial domain, while the random field model considers the spatial variability of structural parameters. For both random variable and random field models, different formulations and the related eigenvalue solution techniques have been developed.

In recent years, stochastic finite element method (SFEM) [10–14] has been widely used in stochastic structural analysis. In this method, a finite number of random variables is used to replace the random fields with element properties, and a Gaussian probability model with uncertainties of parameters and boundary conditions can be established to solve eigenvalue problems. Based on this idea, researchers have developed a variety of stochastic finite element methods based on random field discretization. These random field discretization methods can be largely classified into three groups: (i) spatial discretization such as local averages [15] or mid-point method [16]; (ii) spectral discretization such as Karhunen-Loève (KL) expansion [17] or other orthogonal expansions for the random fields [18] and optimal linear estimation-based methods [19]; (iii) shape function discretization such as using stochastic shape functions [20] or weighted integrals method [21]. The eigenvalue problems corresponding to stochastic finite element models can be expressed as the generalized stochastic eigenvalue problem[22]. We refer to the review paper [23–31] for a variety of technologies and algorithms for stochastic eigenvalue problems. Then the statistics of eigensolutions can be computed by using a range of different stochastic solution techniques, which include, but are not limited to, (1) Monte Carlo simulation based methods [32], (2) perturbation methods [7, 33], (3) surrogate model based techniques such

as polynomial chaos (PC) [32], (4) hybrid methods [34], (5) iterative methods [35] and asymptotic methods [3, 36]. The random field model based on stochastic finite element method and the related algorithms have significantly contributed to the field of stochastic eigenvalue problems for engineering applications. However, the research status of stochastic eigenvalue analysis using stochastic finite element method is shown in Fig.1. The solution of the stochastic eigenvalue problem can be concerned from the following three aspects: 1) the complexity of the structure to be solved, 2) the frequency range to be solved, and 3) the dimension of the random parameters. For stochastic analysis, the effect of uncertainty is significant in the higher frequency ranges. As the wavelength shrinks over the higher frequency range, a very fine mesh size is required to accurately represent the dynamic behavior, which greatly increases the computational effort. In addition, for complex built-up structures with multiple random structural parameters, a large number of finite element elements are also needed to obtain the exact solution because one element cannot be used to simulate any continuous and uniform part of the structure. In these cases, the SFEM solution may be expensive or infeasible from a computational standpoint. High-frequency stochastic eigenvalue analysis of complex structures is affected by mesh density, computation amount and accuracy, which is an area that cannot be covered by finite element. As Fig.1 shows, stochastic analysis requires an appropriate approach to avoid these limitations and effects.
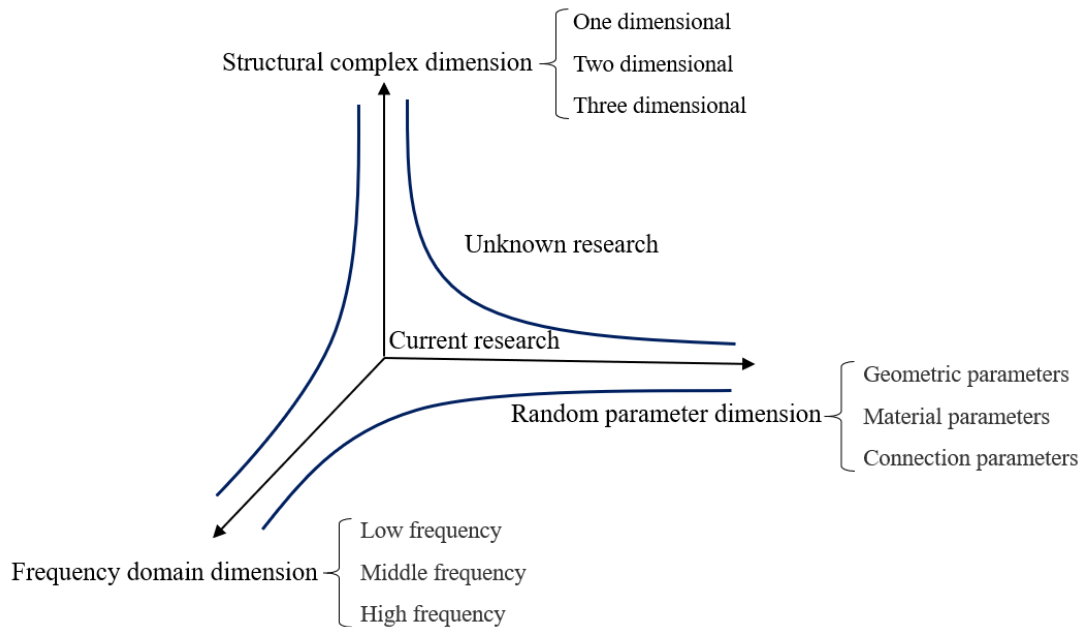

Fig. 1: The research field of stochastic eigenvalues

A powerful tool to fill this gap is the dynamic stiffness method (DSM) [37–40]. The method is often referred to as an exact method as it is based on exact general solution of the governing differential equations. The method provides the analysts with much better model accuracy when compared to finite element or other approximate methods. This is because the analysis accuracy of DSM is independent of the number of elements used in the analysis. The elegance of the method becomes apparent when higher frequencies and

higher accuracy of results are required. The stochastic dynamic stiffness(SDS) models for two-dimensional structures such as membranes have recently been developed by the authors[41]. The SDS models not only have the merits of the dynamic stiffness method that are accurate for the whole frequency by using very few DOFs but also consider the parameter uncertainties in the model to allow stochastic analysis. Based on these SDS models, broadband dynamic response analyses have been carried out for both beam structures[42] and membrane built-up structures[41]. However, to the best knowledge of the authors, there has no research on the eigenvalue solution techniques that enable one to extract eigensolutions from the analytically expressed SDS formulations.

In this paper, an effective and reliable eigenvalue solution technique is proposed to extract both stochastic eigenvalues and mode shapes from analytical stochastic dynamic stiffness(SDS) formulations with parameter uncertainties. The SDS formulations are developed based on both random variable model and random field model to quantify the uncertainties related to system parameters (such as Young's modulus, mass density and Poisson's ratio). In particular, the KL expansion [10] is used to discrete the random fields in conjunction with frequency-dependent shape function, the elemental SDS matrices for structure members are derived in an analytical manner. Then, the WW algorithm is used to solve the eigenvalues under the deterministic parameters, and the proper mode shape computation technique is used to solve the eigenvectors based on deterministic model. After that, the deterministic eigenvalues and eigenvectors are used as the initial solutions, and the numerical perturbation method based on the inverse iteration method combined with the homotopy algorithm is used to iteratively compute the stochastic eigenvalues and eigenvectors. In general, this work combines the merits of both the KL spectral expansion and DSM mentioned above, and proposes an accurate and efficient numerical perturbation method which provides a powerful efficient and accurate tool for stochastic eigenvalue analysis of built-up structures such as beam, plate and beam-plate built-up structures.

In the rest of this paper, Section 2 presents the stochastic dynamic stiffness formulations based on both random variable model and random field model. Then, Section 3 describes the stochastic eigenvalue solution techniques. In more specific, Sections 3.1 reviews the Wittrick-Williams algorithm and mode shape computation techniques for deterministic DS models. A numerical perturbation method based on inverse iteration for solving the stochastic stiffness matrix is proposed in detail in Section 3.2. In Section 4, the proposed analysis method is applied to the beam built-up structures by using Monte Carlo simulations which are compared with those from other results such as from stochastic finite element models. Finally, Section 5 concludes the paper.

2. Stochastic dynamic stiffness(SDS) formulation for beam built-up structures with parameters uncertainty

The governing differential equation of a linear structural system with stochastic parameter uncertainties, subjected to external excitations is most often a set of linear differential equation with random coefficients. The problem can be stated as finding the solution of equation

$$\mathrm{L}(\Omega, \mathrm{r}, t)\boldsymbol{u}(\Omega, \mathrm{r}, t) = \boldsymbol{f}(\Omega, \mathrm{r}, t) \tag{1}$$

with prescribed boundary conditions and initial conditions. In the above equation L is a linear stochastic differential operator, $\boldsymbol{u}$ is the random system response to be determined, $\boldsymbol{f}$ is the dynamic excitation which can be random, r is the spatial coordinate vector, t is the time and Ω is the sample space denoting the stochastic nature of the problem. Eq. (1) with L as a deterministic operator and $\boldsymbol{f}$ as a random forcing function, has been studied extensively within the scope of random vibration theory [43]. Here our interest is when the operator L itself is random. There are mainly two methods to model parametric uncertainty using the probabilistic approach: (a) uncertainty modeling using random variables, and (b) uncertainty modeling using random fields.
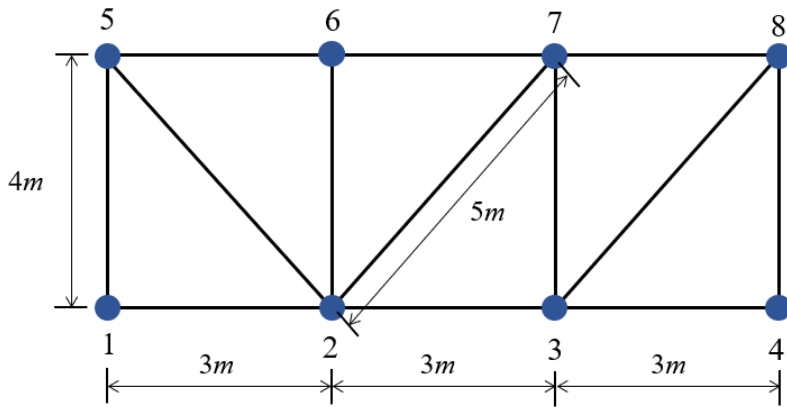

Fig. 2: A beam built-up structure with node 1 clamped

(a) Random variable model
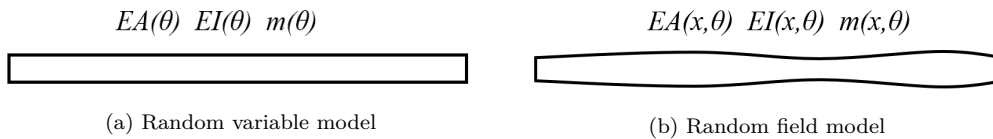
(b) Random field model

Fig. 3: The cross-section parameters random variable model and random field model of each beam member

In order to illustrate the difference of between a random variable and a random field, we introduce a beam built-up structure as shown in Fig. 2. It is composed of 13 different beam members jointed at 8 nodes. The essential cross-section parameters of a beam member include the axial stiffness $EA(x)$, bending stiffness $EI(x)$, and mass $m(x)$, where x is the local coordinate of each beam. The random variable model and random field model of cross-section parameters of each beam member can be demonstrated in Figs. 3(a) and (b) respectively.

In particular for the random variable model as shown in Fig.3(a), the cross-section parameters $AE(\theta)$, $m(\theta)$ and $EI(\theta)$ of each beam member are constant (i.e. uniform cross-section). These parameters of those 13 beam members could be independent of

each other and each item has the following form

$$AE(\theta) = AE_0 \left[1 + \epsilon_{AE}H_{AE}(\theta)\right] \tag{2}$$

$$m(\theta) = m_0[1 + \epsilon_m H_m(\theta)] \tag{3}$$

$$EI(\theta) = EI_0 \left[1 + \epsilon_{EI}H_{EI}(\theta)\right] \tag{4}$$

The 'strength parameters' ϵ_{AE}, ϵ_m, ϵ_{EI} effectively quantify the amount of uncertainty in the axial stiffness, mass per unit length and bending stiffness of beam. The constants AE_0, m_0 and EI_0 are respectively the axial stiffness, mass per unit length and bending stiffness of the underlying baseline model. $H(\theta)$ is assumed to be the random process which is the random number set with Gaussian distribution.

For random field model as shown in Fig.3(b), the cross-section parameters $AE(x,\theta)$, $m(x,\theta)$ and $EI(x,\theta)$ are continuously changed as the local coordinate x changes and each item has the following form

$$AE(x,\theta) = AE_0 \left[1 + \epsilon_{AE}H_{AE}(x,\theta)\right] \tag{5}$$

$$m(x,\theta) = m_0[1 + \epsilon_m H_m(x,\theta)] \tag{6}$$

$$EI(x,\theta) = EI_0 \left[1 + \epsilon_{EI}H_{EI}(x,\theta)\right] \tag{7}$$

where $H(x,\theta)$ is assumed to be the random field associated with the local coordinates.

Stochastic dynamic stiffness formulations are developed for beam member structures based on both random variable and random field in Sections 2.1 and 2.2, respectively. The assembly procedure of beam built-up structures considering axial and bending vibration is described in Section 2.3.

2.1. SDS formulation for a beam member based on random variable modal

Based on the above two random models, the corresponding stochastic dynamic stiffness(SDS) formulations can be derived. For the random variable model, because the cross-section parameters $AE(\theta)$, $m(\theta)$ and $EI(\theta)$ of each beam element are constant, they can be directly introduced into the classical dynamic stiffness formulations of the structure in the following form

$$\boldsymbol{f}_l^a = \boldsymbol{D}_l^a(\omega,\theta)\boldsymbol{d}_l^a \quad \boldsymbol{f}_l^b = \boldsymbol{D}_l^b(\omega,\theta)\boldsymbol{d}_l^b \tag{8}$$

where $\boldsymbol{D}_l^a(\omega,\theta)$ and $\boldsymbol{D}_l^b(\omega,\theta)$ are the dynamic stiffness matrices considering axial vibration and bending vibration in the local coordinate system respectively and the cross-section parameters are essentially random variables. $\boldsymbol{f}_l^a$, $\boldsymbol{d}_l^a$ and $\boldsymbol{f}_l^b$, $\boldsymbol{d}_l^b$ are the force and displacement matrices considering axial vibration and bending vibration in the local coordinate system respectively. Since the derivation process is very mature, interested readers are referred [37–39].

2.2. SDS formulation for a beam member based on random field model

The derivation of the stochastic dynamic stiffness formulation based on the random field model is more complicated. Section 2.2.1 describes the spectral discretization of the random fields. Next, Sections 2.2.2 and 2.2.3 provide respectively the SDS formulations for axial and bending vibration of a beam member.

2.2.1. Random field discretization

Assume that all structural parameters are treated as a Gaussian random field $H(x, \theta)$ with an exponentially decaying autocorrelation function.

$$C(x_1, x_2) = e^{-c|x_1 - x_2|} \tag{9}$$

where the quantity c is inversely proportional to the correlation length. The random field $H(x, \theta)$ can be expanded by using the Karhunen-Loève(KL) expansion in the interval $-l \leq x \leq l$ as

$$H(x, \theta) = \sum_{j=1}^{\infty} \xi_j(\theta) \sqrt{\lambda_j} \varphi_j(x) \tag{10}$$

where $\xi_j(\theta)$ are uncorrelated random coefficients, λ_j and $\varphi_j(x)$ are eigenvalues and eigenfunctions. Since $H(x, \theta)$ is assumed to be a Gaussian random field, without any loss of generality we assumed the mean to be zero, thus the eigenvalues and eigenfunctions in the KL expansion for odd j are given by

$$\lambda_j = \frac{2c}{\alpha_j^2 + c^2}, \qquad \varphi_j(x) = \frac{\cos(\alpha_j x)}{\sqrt{l + \frac{\sin(2\alpha_j l)}{2\alpha_j}}}, \qquad \text{where} \quad \tan(\alpha_j l) = \frac{c}{\alpha_j}, \tag{11}$$

and for even j

$$\lambda_j = \frac{2c}{\alpha_j^2 + c^2}, \qquad \varphi_j(x) = \frac{\sin(\alpha_j x)}{\sqrt{l - \frac{\sin(2\alpha_j l)}{2\alpha_j}}}, \qquad \text{where} \quad \tan(\alpha_j l) = \frac{\alpha_j}{-c}. \tag{12}$$

These eigenvalues and eigenfunctions in the KL expansion will be used to obtain the stochastic elemental mass and stiffness matrices. For all practical purposes, the infinite series in Eq. (10) needs to be truncated at a finite number of terms. The number of terms could be selected based on the 'amount of information' to be retained. This in turn can be related to the number of eigenvalues retained, since the eigenvalues, λ_j, in Eq. (10) are arranged in a decreasing order. For example, if 90% of the information is to be retained, then one can choose the number of terms, N, such that $\lambda_N/\lambda_1 = 0.1$. The value of N mainly depends on the correlation length of the underlying random field. One needs more terms when the correlation length is small. Intuitively this means that more independent variables are needed for fields with smaller correlation lengths and vice versa.

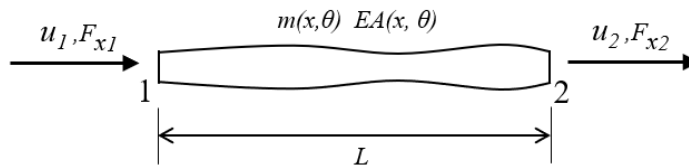## 2.2.2. SDS formulation for axial vibration of a stochastically inhomogeneous bar member

Fig. 4: Axial vibration of a bar member, where the axial stiffness $EA(x, \theta)$ and mass per unit length $m(x, \theta)$ are assumed to be random fields.

The governing differential equation for a stochastically inhomogeneous bar under axial vibration is given as follows

$$\frac{\partial}{\partial x}\left[AE(x)\frac{\partial U(x,t)}{\partial x}\right] = m(x)\frac{\partial^2 U(x,t)}{\partial t^2} \tag{13}$$

where $U(x,t)$ is the axial displacement. The axial stiffness $AE(x,\theta)$ and the mass per unit length $m(x,\theta)$ are assumed to be random fields taking the form of Eqs. (5)-(6).

Next, we need to use the shape function $N(x,\omega)$ to derive the deterministic and random part of the elemental matrices, i.e., the elemental stiffness and the mass matrices. we can express these matrices as [39]

$$\mathbf{K}^a(\omega,\theta) = \mathbf{K}_0^a(\omega) + \Delta\mathbf{K}^a(\omega,\theta), \mathbf{M}^a(\omega,\theta) = \mathbf{M}_0^a(\omega) + \Delta\mathbf{M}^a(\omega,\theta) \tag{14}$$

The deterministic stiffness and mass matrix can be obtained from equation as

$$\mathbf{K}_0^a(\omega) = \mathbf{\Gamma}(\omega)\widetilde{\mathbf{K}}_0^a(\omega)\mathbf{\Gamma}^T(\omega), \mathbf{M}_0^a(\omega) = \mathbf{\Gamma}(\omega)\widetilde{\mathbf{M}}_0^a(\omega)\mathbf{\Gamma}^T(\omega) \tag{15}$$

To obtain the matrices associated with the random components, note that for each j there will be two different matrices corresponding to the two eigenfunctions in Eqs. (11)-(12). $\Delta\mathbf{K}^a(\omega,\theta)$ and $\Delta\mathbf{M}^a(\omega,\theta)$ are the random part of the matrices which can be conveniently expressed as

$$\Delta\mathbf{K}^a(\omega,\theta) = \mathbf{\Gamma}(\omega)\Delta\widetilde{\mathbf{K}}^a(\omega,\theta)\mathbf{\Gamma}^T(\omega), \Delta\mathbf{M}^a(\omega,\theta) = \mathbf{\Gamma}(\omega)\Delta\widetilde{\mathbf{M}}^a(\omega,\theta)\mathbf{\Gamma}^T(\omega) \tag{16}$$

The matrix $\Delta\widetilde{\mathbf{K}}^a(\omega)$ and $\Delta\widetilde{\mathbf{M}}^a(\omega)$ can be expanded by utilizing the Karhunen-Loève expansion as

$$\Delta\widetilde{\mathbf{K}}^a(\omega,\theta) = \sum_{j=1}^{M_K} \xi_{K_j}(\theta)\sqrt{\lambda_{K_j}}\widetilde{\mathbf{K}}_j^a(\omega), \Delta\widetilde{\mathbf{M}}^a(\omega,\theta) = \sum_{j=1}^{M_K} \xi_{M_j}(\theta)\sqrt{\lambda_{M_j}}\widetilde{\mathbf{M}}_j^a(\omega) \tag{17}$$

where $\sqrt{\lambda_{K_j}}$ and $\sqrt{\lambda_{M_j}}$ are the eigenvalues corresponding to the random field. The derivation of the matrices $\widetilde{\mathbf{K}}_j^a(\omega)$ and $\widetilde{\mathbf{M}}_j^a(\omega)$ are given in the Appendix A. Finally, the stochastic dynamic stiffness matrix $\mathbf{D}_l^a(\omega,\theta)$ for the axial vibration of a bar member under local coordinates can be obtain as

$$\mathbf{D}_l^a(\omega,\theta) = -\omega^2\mathbf{M}^a(\omega,\theta) + \mathbf{K}^a(\omega,\theta) \tag{18}$$

such that $\boldsymbol{f}_l^a = \mathbf{D}_l^a(\omega,\theta)\boldsymbol{d}_l^a$, where $\boldsymbol{f}_l^a = [F_{x_1}, F_{x_2}]^T$, $\boldsymbol{d}_l^a = [u_1, u_2]^T$, where F_x with suffices 1 and 2 represent the axial force at the two end nodes (1 and 2) of the bar member; u with suffices 1 and 2 represent amplitudes of the axial displacement of the bar cross-section at the two end nodes of the bar member.

2.2.3. SDS formulation for bending vibration of a stochastically inhomogeneous beam member

The governing differential equation for a stochastically inhomogeneous Euler-Bernoulli beam under bending vibration is given by

$$\frac{\partial^2}{\partial x^2}\left[EI(x)\frac{\partial^2 W(x,t)}{\partial x^2}\right] + m(x)\frac{\partial^2 W(x,t)}{\partial t^2} = 0 \tag{19}$$
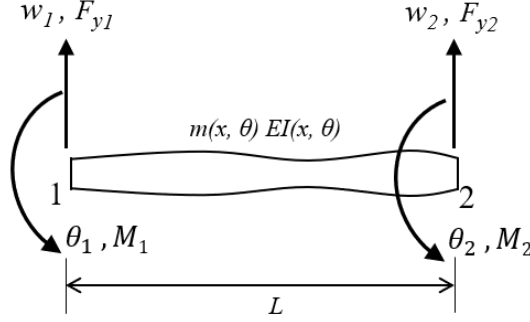
Fig. 5: Bending vibration of a beam member, where the bending stiffness $EI(x, \theta)$ and mass per unit length $m(x, \theta)$ are assumed to be random fields.

where $W(x, t)$ is the transverse flexural displacement. The mass per unit length $m(x, \theta)$ and the bending stiffness $EI(x, \theta)$ are assumed to be random fields of the form given by Eqs. (6)-(7).

Next, we need to use the shape function $\mathrm{N}(x, \omega)$ to derive the deterministic and random part of the elemental matrices. Like the axial vibration of beam, the elemental stiffness and mass matrices are given in Appendix B (It should be noted that there are many mistakes in the explicit expressions for the elemental stiffness and mass matrices in Ref.[42], which have all been corrected in the Appendix B). Finally, the stochastic dynamic stiffness matrix $\mathbf{D}_l^b(\omega, \theta)$ for the bending vibration of a beam can be given as

$$\mathbf{D}_l^b(\omega, \theta) = -\omega^2 \mathbf{M}^b(\omega, \theta) + \mathbf{K}^b(\omega, \theta) \tag{20}$$

such that $\boldsymbol{f}_l^b = \mathbf{D}_l^b(\omega, \theta)\boldsymbol{d}_l^b$, where $\boldsymbol{f}_l^b = [F_{y_1}, M_1, F_{y_2}, M_2]^{\mathrm{T}}$, $\boldsymbol{d}_l^b = [w_1, \theta_1, w_2, \theta_2]^{\mathrm{T}}$, where F_y and M with suffices 1 and 2 represent the shear force, and bending moment at the two end nodes (1 and 2) of the beam member, respectively; w and θ with suffices 1 and 2 represent amplitudes of the vertical and bending displacement, and the angular or bending rotation of the beam cross-section at the two end nodes of the beam member, respectively.

2.3. The assembly procedure of SDS elements for stochastically inhomogeneous beam built-up structures

A stochastically inhomogeneous beam member under axial and bending vibration is shown in Fig. 6. The elemental stochastic dynamic stiffness matrix $\mathbf{D}_l^e(\omega)$ of a beam member in local coordinate can be written in the form

$$\boldsymbol{f}_l^e = \mathbf{D}_l^e(\omega, \theta)\boldsymbol{d}_l^e \tag{21}$$

where

$$\boldsymbol{f}_l^e = [F_{x1}, F_{y1}, M_1, F_{x2}, F_{y2}, M_2]^{\mathrm{T}} \quad \boldsymbol{d}_l^e = [u_1, w_1, \theta_1, u_2, w_2, \theta_2]^{\mathrm{T}} \tag{22}$$
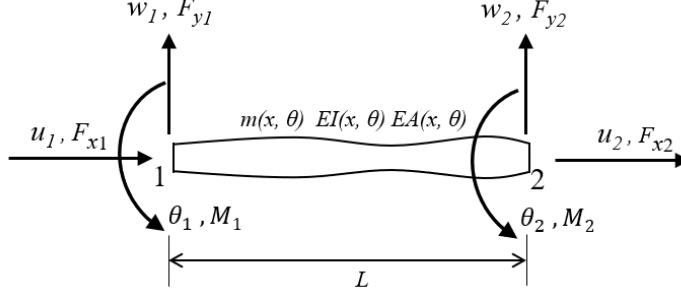
Fig. 6: Both axial and bending vibrations of a beam member, where the bending stiffness $EI(x,\theta)$, mass per unit length $m(x,\theta)$ and axial stiffness $AE(x,\theta)$ are assumed to be random fields.

$$\mathbf{D}_l^e(\omega,\theta) = \begin{bmatrix} \mathbf{D}_{l_{11}}^a & 0 & 0 & \mathbf{D}_{l_{12}}^a & 0 & 0 \\ 0 & \mathbf{D}_{l_{11}}^b & \mathbf{D}_{l_{12}}^b & 0 & \mathbf{D}_{l_{13}}^b & -\mathbf{D}_{l_{14}}^b \\ 0 & \mathbf{D}_{l_{21}}^b & \mathbf{D}_{l_{22}}^b & 0 & -\mathbf{D}_{l_{23}}^b & \mathbf{D}_{l_{24}}^b \\ \mathbf{D}_{l_{21}}^a & 0 & 0 & \mathbf{D}_{l_{22}}^a & 0 & 0 \\ 0 & \mathbf{D}_{l_{31}}^b & -\mathbf{D}_{l_{32}}^b & 0 & \mathbf{D}_{l_{33}}^b & -\mathbf{D}_{l_{34}}^b \\ 0 & -\mathbf{D}_{l_{41}}^b & \mathbf{D}_{l_{42}}^b & 0 & -\mathbf{D}_{l_{43}}^b & \mathbf{D}_{l_{44}}^b \end{bmatrix} \tag{23}$$

where F_x, F_y and M with suffices 1 and 2 represent the axial force, shear force, and bending moment at the two end nodes (1 and 2) of the beam member, respectively; u, w and θ with suffices 1 and 2 represent amplitudes of the axial displacement, the vertical and bending displacement, and the angular or bending rotation of the beam cross-section at the two end nodes of the beam member, respectively, where the coefficients $\mathbf{D}_l^a(\omega,\theta)$ and $\mathbf{D}_l^b(\omega,\theta)$ have been given in Eqs. (18) and (20). Finally, the stochastic dynamic stiffness matrix $\mathbf{D}_g^e(\omega,\theta)$ of a beam member in the global coordinate can be given as

$$\mathbf{D}_g^e(\omega,\theta) = \boldsymbol{T}\mathbf{D}_l^e(\omega,\theta)\boldsymbol{T}^{\mathrm{T}} \tag{24}$$

where $\boldsymbol{T}$ is the transfer matrix taking the form

$$\boldsymbol{T} = \begin{bmatrix} Ct & St & 0 & 0 & 0 & 0 \\ -St & Ct & 0 & 0 & 0 & 0 \\ 0 & 0 & 1 & 0 & 0 & 0 \\ 0 & 0 & 0 & Ct & St & 0 \\ 0 & 0 & 0 & -St & Ct & 0 \\ 0 & 0 & 0 & 0 & 0 & 1 \end{bmatrix} \tag{25}$$

where $Ct = \cos(\varphi)$ and $St = \sin(\varphi)$, and φ is the angle of the beam member as shown in Fig. 7 (from node 1 to node 2) in the global coordinate system. Then, the elemental SDS matrices can be assembled directly to form the overall SDS matrix of the final built-up structure.

3. Stochastic eigenvalue solution techniques for stochastic dynamic stiffness formulations

In Section 2, we have developed the stochastic dynamic stiffness (SDS) formulations for beam built-up structures based on both the random variable and random field models.
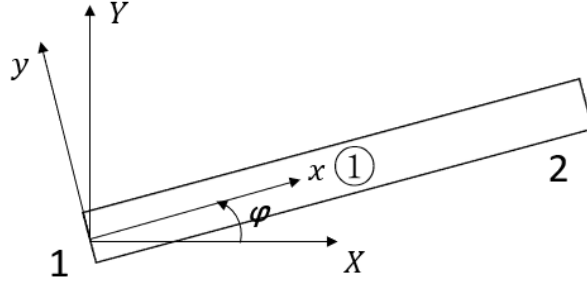
Fig. 7: A beam member in the global coordinate system.

Then the stochastic eigenvalues and mode shapes can be extracted from the analytically formulated SDS matrices. It is worth noting that the stochastic eigenvalue problems in the form of analytical SDS formulations are essentially transcendental functions of frequencies. Therefore the normal used linear algebraic solvers like Lanczos method is not applicable any more, and it is necessary to propose the corresponding solution techniques for these analytical SDS formulations. This section mainly devotes to two eigenvalue solution techniques and the associated mode shape computation techniques for those dynamic stiffness formulations. As illustrated in Table 1, the well-known Wittrick-Williams(WW) algorithm is applicable to both deterministic DS formulations and the SDS formulations based on random variable models, but is not applicable to the SDS formulations based on random field models as described in Section 2.2. Under this background, a numerical perturbation method(NPM) based on inverse iteration with high robustness and high efficiency is proposed for extracting eigensolutions from stochastic dynamic stiffness(SDS) formulations based on both random variable models and random field models with the whole frequency range. It should be mentioned by passing that the proposed NPM is numerical perturbation method based on both the eigenvalues and eigenvectors computed by the WW algorithm and the corresponding mode shape computation technique. Therefore, it is very critical that both the eigenvalues and eigenvectors extracted from the baseline model should be accurate and reliable. Next, in Section 3.1, we first present the highly robust, efficient and accurate WW algorithm and the associated mode shape computation technique, then followed by the proposition of the NPM in Section 3.2.

Table 1: The application of Wittrick-Williams(WW) algorithm and numerical perturbation method(NPM) for different dynamic stiffness formulations

DS formulations	Solution techniques	
	WW algorithm	NPM
Deterministic	$\checkmark$	Not necessary
Random variable	$\checkmark$	$\checkmark$
Random field	$\times$	$\checkmark$

3.1. Wittrick-Williams algorithm for eigenvalue computation and mode shape computation technique

Both the deterministic dynamic stiffness(DS) formulations and the SDS formulations based on random variable models are transcendental functions of frequency where its elements are trigonometric and hyper-trigonometric functions of frequency. A reliable and efficient solution technique to extract eigenvalue of natural frequencies from the analytical deterministic DS formulations of a structure is the powerful Wittrick-Williams (WW) algorithm [44]. This algorithm ensures that no eigenvalue is missed by monitoring the Sturm sequence of the ensuring matrix. According to the WW algorithm, the number of eigenvalues between 0 and a trial frequency ω^* (mode count J) of the final structure is

$$J = J_0 + s\{\mathbf{K}_f\} \tag{26}$$

where J_0 count is mode count of an element with all nodes clamped, and $s(\mathbf{K}_f)$ is the sign count (negative inertia) of the final structure $\mathbf{K}_f$ evaluated at the trial frequency. For convenience, the natural frequencies of any member with both ends clamped are denoted by ω_c and are called member clamped-clamped frequencies, with the corresponding modes being called local ones. And $J_0 = \sum J_m$, where J_m is the number of ω_c of a member subject to $\omega_c \leq \omega^*$, and the summation is over all members. By applying the bisection method, the eigenvalues where the mode count J shifts can be determined. It is worth emphasis that the WW algorithm [44], which has been used in many DS formulations, e.g., [45–49]. The WW algorithm is probably the most suitable solution technique for dynamic stiffness models with the following advantages

i) Accuracy: Eigenvalues within any required precision can be computed;
ii) High efficiency: It is highly efficient mainly due to the small-size matrix;
iii) Analytical elegance: Infinite eigenvalues can be extracted from finite dimensional matrix;
iv) Certainty: The algorithm ensures that no eigenvalue will be missed.

However, the advantages of ii), iii) and iv) can be realized only when the key problem of the so called J_0 count (the mode count of all fully clamped members) in the WW algorithm can be effectively solved; Otherwise, either some spurious modes will enter into the calculation or some true modes will be missed, so that the advantage of the above iv) certainty cannot be fully realized. However, in the SDS formulations based on the random field model, the J_0 count is not likely to be deduced since the SDS matrices of each elements are essentially the superposition of many stochastic components as evident in Eq. (23) and Appendices A and B. Therefore, for such SDS formulations, a new solution technique will be proposed in Section 3.2.

Once an eigenvalue is obtained, the corresponding eigenvectors(mode shapes) can be computed. As mentioned earlier, considering that Monte Carlo simulation in random problems requires a large number of samples, it is very important to select the most reliable and fast computational technique. Here, based on the criteria suggested [50], four main different mode shape computation techniques are compared and contrasted in Table 2, include, (M1) Let the last (or a chosen) element of the eigenvector $\boldsymbol{u}_0$ be an arbitrary value, and calculate the rest elements. (M2) Let the last h-1 elements of the eigenvector $\boldsymbol{u}_0$ null and the hth from last element having an arbitrary value, where h is

the distance up the diagonal of dynamic stiffness matrix $\mathbf{K}^\Delta$ changing through the upper triangle to its lowest negative element. (M3) For the form containing the external force P, the eigenvector $\boldsymbol{u}_0$ can be directly obtained from $P \times \mathbf{K}^{-1}$. (M4) The transcendental eigenvalue problem is first reduced to a generalized linear eigenvalue problem by using Newton's method in the vicinity of an exact natural frequency identified by the Wittrick–Williams algorithm. Then the exact eigenvectors can be obtained by using standard inverse iteration or subspace iteration.

Table 2: Comparison of four main mode shapes computation techniques. Note that for an element of subjective judgement is used to score from one-star to four-star.

Criterion	Method			
	M1	M2	M3	M4
Simple	★ ★ ★ ★	★ ★ ★	★ ★	★
Fast	★ ★ ★	★ ★ ★	★	★ ★ ★ ★
Cheap	★ ★ ★ ★	★ ★ ★ ★	★ ★ ★	★ ★
Accurate	★ ★	★ ★	★ ★	★ ★ ★ ★
Reliable	★	★	★ ★	★ ★ ★ ★

This paper uses the M4 method for mode shapes computation. The M4 method applies Newton's method see Eq.(27), expanding the approximation $\omega_a \in (\omega_l, \omega_u)$ of $\mathbf{K}(\omega_k)\boldsymbol{d}_k = 0$ with respect to the eigenvalue ω_k.

$$\mathbf{K}(\omega_k)\boldsymbol{d}_k = \mathbf{K}_a\boldsymbol{d}_k + (\omega_k - \omega_a)\mathbf{K}'_a\boldsymbol{d}_k + O((\omega_k - \omega_a)^2) \qquad (27)$$

where $\mathbf{K}_a = \mathbf{K}(\omega_a)$, $\mathbf{K}'_a = d\mathbf{K}(\omega_a)/d\omega$. Note that $\mathbf{K}(\omega_k)\boldsymbol{d}_k = 0$, ignoring the second order and higher order terms, the natural frequency ω_k and eigenvector $\boldsymbol{d}_k$ can be obtained by solving the generalized matrix eigenvalue problem

$$\mathbf{K}_a\boldsymbol{d} = \tau\mathbf{K}'_a\boldsymbol{d} \qquad (28)$$

where $\tau = \omega_a - \omega_k$. The method to solve the generalized matrix eigenvalue problem is the inverse power iteration method commonly used in the linear matrix eigenvalue problem. According to Eq.(28), we can get the following form

$$\bar{\boldsymbol{d}}^{(i+1)} = \mathbf{K}_a^{-1}\mathbf{K}'_a\boldsymbol{d}^{(i)} \qquad (29)$$

where i is the number of steps of iteration, and the $\boldsymbol{d}^{(0)}$ is a random vector. Then the updated $\tau^{(i+1)}$ can be obtained by

$$\tau^{(i+1)} = \frac{1}{\bar{\mathrm{d}}_{j^*}^{(i+1)}} \qquad (30)$$

where $|\bar{\mathrm{d}}_{j^*}^{(i+1)}| = \max |\bar{\mathrm{d}}_j^{(i+1)}|$. Finally, the updated eigenvector $\mathbf{d}^{(i+1)}$ is obtained by

$$\mathbf{d}^{(i+1)} = \tau^{(i+1)}\bar{\mathbf{d}}^{(i+1)} \qquad (31)$$

The whole iterative process is terminated when

$$\max \left|\mathrm{d}_j^{(i+1)} - \mathrm{d}_j^{(i)}\right| < \mathrm{Tol}\,1 \text{ or } i = i_{\max} \qquad (32)$$

where $d_j^{(i)}$ is the jth element of $\mathbf{d}^{(i)}$, max denotes the maximum value for any j, Tol 1 is the user specified error tolerance. $i_{\max}$ is the maximum number of iterations allowed. It's worth noting that since $\mathbf{d}^{(i)}$ has been normalized, only absolute error control is used in Eq.(32). This method can ensure the convergence to the eigenvalue and eigenvector with the minimum absolute value. The complete algorithm steps of this method are given in reference [50]. The above WW algorithm and the mode shapes computational technique can be applied to both deterministic DS formulations and stochastic DS formulations based on random variable models, but can not be applied to stochastic DS formulations based on random field models.

3.2. Numerical perturbation method for stochastic DS formulations

The numerical perturbation method based on inverse iteration can be used to solve the stochastic dynamic stiffness formulations based on both random variable and random field models. It provides a powerful solution for the dynamic stiffness method to solve stochastic problems. The derivation process is described in detail below. The numerical perturbation method needs to take the deterministic eigenvalues and eigenvectors as the basis of iteration, based on deterministic dynamic stiffness formulation, the deterministic eigenvalue problem can be written as

$$\mathbf{K}(\omega_0, \mathrm{x}_0)\boldsymbol{u}_0 = 0 \tag{33}$$

where $\mathbf{K}$ is the deterministic dynamic stiffness matrix of the structure, ω_0 denotes the deterministic eigenvalue, $\mathrm{x}_0 \in \mathbb{C}^{N \times 1}$ represents the deterministic parameter vector and $\boldsymbol{u}_0$ is the corresponding deterministic eigenvector for displacement amplitude. Note that both ω_0 and $\bar{\boldsymbol{u}}_0$ have already been determined by the procedure given in Section 3.1, thus can be treated as constants in the following stochastic eigenvalue analysis.

Without any loss of generality, if uncertainties are considered in the dynamic stiffness model, the stochastic dynamic stiffness formulation becomes

$$\mathbf{K}(\omega_0 + \mathrm{d}\omega(\mathrm{dx}), \mathrm{x}_0 + \mathrm{dx})(\boldsymbol{u}_0 + \mathrm{d}\boldsymbol{u}(\mathrm{dx})) = 0 \tag{34}$$

which covers both the random variable models and random field models. It should be noted that compared to the deterministic model, the perturbation on the eigenvalue ω_0 and eigenvector $\boldsymbol{u}_0$, i.e., $\mathrm{d}\omega$ and $\mathrm{d}\boldsymbol{u}$ are nonlinear functions of the perturbation of parameter vector dx. Therefore, the homotopy method is used to obtain eigenvalues and eigenvectors, The specific form is as follows:

$$\mathrm{x}_0 = 0, \mathrm{x}_1, \cdots, \mathrm{x}_k, \cdots, \mathrm{x}_M = \mathrm{x}_g, \qquad \text{where} \quad \mathrm{x}_k = k(\mathrm{x} - \mathrm{x}_0)/M \tag{35}$$

$$\omega_0, \omega_1, \cdots, \omega_k, \cdots, \omega_M = \omega_g, \qquad \text{where} \quad \omega_k = k(\omega - \omega_0)/M \tag{36}$$

$$\boldsymbol{u}_0, \boldsymbol{u}_1, \cdots, \boldsymbol{u}_k, \cdots, \boldsymbol{u}_M = \boldsymbol{u}_g, \qquad \text{where} \quad \boldsymbol{u}_k = k(\boldsymbol{u} - \boldsymbol{u}_0)/M \tag{37}$$

where M is the total homotopy number, the value of M can directly affect the convergence of the final stochastic eigenvalues and eigenvectors. For different types of beam, it is necessary to choose the appropriate M to adjust the convergence. k $(k = 0, 1, \cdots, M-1)$ is the step of the current iteration. x_0, ω_0 and $\boldsymbol{u}_0$ are deterministic parameters, eigenvalue and eigenvector. x_k, ω_k, and $\boldsymbol{u}_k$ respectively represent the stochastic parameters,

stochastic eigenvalues and stochastic eigenvectors obtained in each iteration process. x_g, ω_g, and $\boldsymbol{u}_g$ respectively represent the final stochastic parameters and computed stochastic eigenvalues and eigenvectors. The characteristic solution iterated in each step will be used as the initial guess of the next iteration process. At the end of iteration, stochastic eigenvalues and eigenvectors can be obtained. The detailed iterative process of the algorithm is as follows:

For iteration at step k:

The eigenvector is updated by using inverse iteration. First of all, applying Taylor expansion onto Eq.(34) at $\mathbf{K}(\omega_k, \mathrm{x}_{k+1})$, one will have

$$\left[\mathbf{K}(\omega_k, \mathrm{x}_{k+1}) + \frac{\partial \mathbf{K}(\omega_k, \mathrm{x}_{k+1})}{\partial \omega} \mathrm{d}\omega\right] \boldsymbol{u}_{k+1} = 0 \tag{38}$$

where x_{k+1} represents the parameter vector. Eq.(38) can be recast into the following form

$$\mathbf{K}(\omega_k, \mathrm{x}_{k+1})\boldsymbol{u}_{k+1} = -\mathrm{d}\omega\frac{\partial \mathbf{K}(\omega_k, \mathrm{x}_{k+1})}{\partial \omega}\boldsymbol{u}_{k+1} \simeq -\mathrm{d}\omega\frac{\partial \mathbf{K}(\omega_k, \mathrm{x}_{k+1})}{\partial \omega}\boldsymbol{u}_k \tag{39}$$

Therefore, the eigenvector $\boldsymbol{u}_{k+1}$ can be updated by using the inverse iteration to be

$$\begin{aligned}
\bar{\boldsymbol{u}}_{k+1} &= -\mathbf{K}(\omega_k, \mathrm{x}_{k+1})^{-1}\left(\mathrm{d}\omega\frac{\partial \mathbf{K}(\omega_k, \mathrm{x}_{k+1})}{\partial \omega}\right)\boldsymbol{u}_k \\
&= -\mathbf{K}(\omega_k, \mathrm{x}_{k+1})^{-1}\left[\mathbf{K}(\omega_k + \mathrm{d}\omega, \mathrm{x}_{k+1}) - \mathbf{K}(\omega_k, \mathrm{x}_{k+1})\right]\boldsymbol{u}_k \\
&= \left[\mathrm{I} - \mathbf{K}(\omega_k, \mathrm{x}_{k+1})^{-1}\mathbf{K}(\omega_k + \mathrm{d}\omega, \mathrm{x}_{k+1})\right]\boldsymbol{u}_k \quad (40)
\end{aligned}$$

Then, the updated eigenvector $\bar{\boldsymbol{u}}_{k+1}$ needs to be normalised to $\boldsymbol{u}_{k+1}$ such that

$$\boldsymbol{u}_{k+1}^{T}\frac{\partial \mathbf{K}(\omega_k, \mathrm{x}_{k+1})}{\partial \omega}\boldsymbol{u}_{k+1} = -1 \tag{41}$$

in order to ensure the convergence of the iteration procedure, namely

$$\boldsymbol{u}_{k+1} = \frac{\bar{\boldsymbol{u}}_{k+1}}{\sqrt{\left|\bar{\boldsymbol{u}}_{k+1}^{T}\frac{\partial \mathbf{K}(\omega_k, \mathrm{x}_{k+1})}{\partial \omega}\bar{\boldsymbol{u}}_{k+1}\right|}} \tag{42}$$

After normalization of the updated eigenvector, the eigenvector $\bar{\boldsymbol{u}}_{k+1}$ for the $k+1$ step is obtained. Then the eigenvalue is updated by using Rayleigh quotient in combination with the iterated eigenvectors. By replacing $\mathrm{d}\omega$ of Eq.(34) by $\Delta\omega_k$, we have

$$\left[\mathbf{K}(\omega_k, \mathrm{x}_{k+1}) + \frac{\partial \mathbf{K}(\omega_k, \mathrm{x}_{k+1})}{\partial \omega}\Delta\omega_k\right] \boldsymbol{u}_{k+1} = 0 \tag{43}$$

thus, by considering Eq.(41), one has

$$\Delta\omega_k = \bar{\boldsymbol{u}}_{k+1}^{T}\mathbf{K}(\omega_k, \mathrm{x}_{k+1})\bar{\boldsymbol{u}}_{k+1} \tag{44}$$

and therefore the updated eigenvalue becomes

$$\omega_{k+1} = \omega_k + \bar{\boldsymbol{u}}_{k+1}^{T}\mathbf{K}(\omega_k, \mathrm{x}_{k+1})\bar{\boldsymbol{u}}_{k+1} \tag{45}$$

Based on the above iterative process, we can obtain the eigenvalues and eigenvectors of $k + 1$ step. Finally, the stochastic eigenvalues and eigenvectors of the stochastic dynamic stiffness formulations based on either random variables or random fields can be computed by using the above technique.

4. Numerical Results and Discussion

The above eigenvalue and mode shape solution technique have been implemented in a Matlab code. Next, we used this code for stochastic analysis of eigenvalue problems in the form of stochastic dynamic formulations based on both random variable model and random field model. Section 4.1 demonstrates modal analysis of the random variable model through the Monte Carlo simulations(MCS). For the SDS formulations for beam built-up structures based on random variable model, both the Wittrick-Williams(WW) algorithm and the numerical perturbation method(NPM) are used in the MCS, in which the eigen-solutions computed by the WW algorithm can be treated as benchmark results. The NPM results are validated against and compared with the results from the WW algorithm, to demonstrate the high accuracy, reliability and efficiency of the NPM. Later in Section 4.2, for the SDS formulations for beam built-up structures based on random field model, the proposed NPM is applied for the stochastic eigenvalue problems, whose results are compared with those by the stochastic finite element method(SFEM).
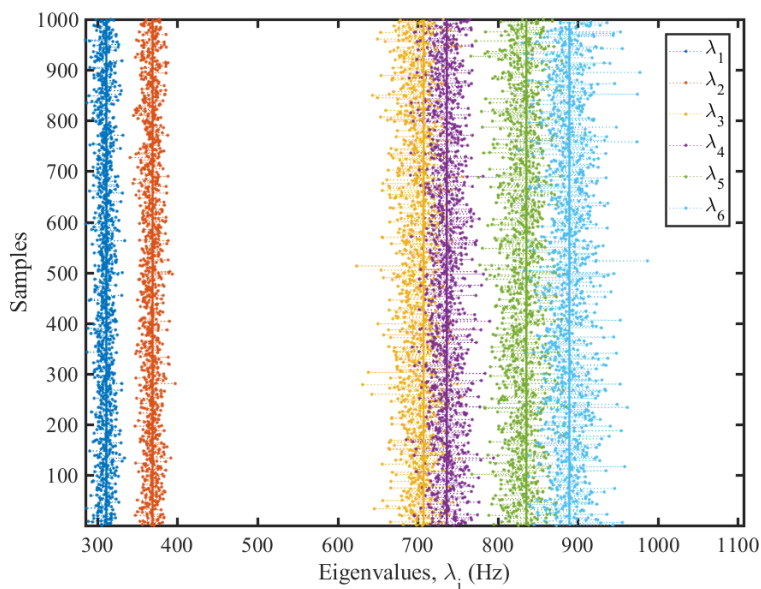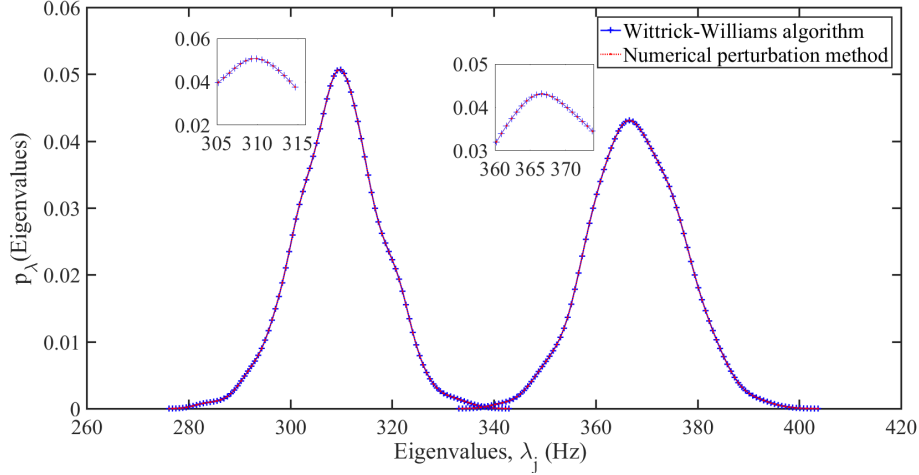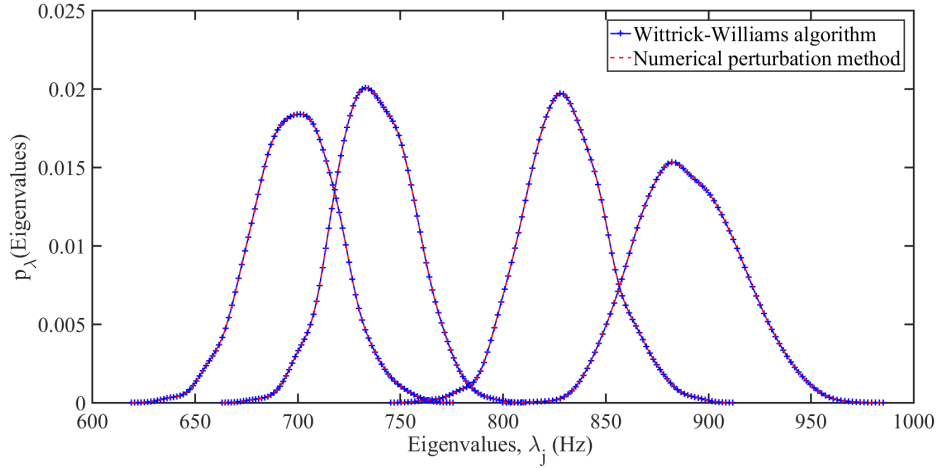
4.1. Modal analysis of the random variable model

Fig. 8: Statistical scatter of the first six eigenvalues of the beam built-up structures shown in Fig. 2 based on random variable models by using numerical perturbation method(NPM). The six vertical continuous lines represent the deterministic eigenvalues for the first six eigenmodes.

This section adopts the beam built-up structures shown in Fig. 2 as an example. The mean material properties are considered $\rho_0 = 2700 \text{kg/m}^3$ and $E_0 = 69 \text{GPa}$. The

area and the area moment of inertia of the cross-section of the underlying baseline model are $A_0 = 1\text{cm}^2$ and $I_0 = 2.876 \times 10^{-11}\text{m}^4$. Node 1 of the beam built-up structures is clamped and the rest nodes are all free. As mentioned in Section 2.1, the $EA(\theta)$, $EI(\theta)$ and $m(\theta)$ are assumed to be uncorrelated, constantly distributed in length, zero-mean, unit-standard-deviation Gaussian random parameters(N(0,1)). The 'strength parameters' ϵ is assumed to be 0.1, that is, we consider 10% randomness for all the parameter values.

(a) Case 1 Probability density functions of the first two stochastic natural frequencies of the beam built-up structures shown in Fig. 2 based on random variable model.

(b) Case 2 Probability density functions of the third to sixth stochastic natural frequencies of the beam built-up structures shown in Fig. 2 based on random variable model.

Fig. 9: Probability density functions of the first six stochastic natural frequencies of the beam built-up structures shown in Fig. 2 based on random variable model by using both Wittrick-Williams(WW) algorithm and numerical perturbation method(NPM).

The statistical scatter of the first six eigenvalues of the beam built-up structures with 1500 samples shown in Fig. 2 based on random variable model by using numerical perturbation method(NPM) is shown in Fig. 8. Solid lines represent the eigenvalues for the corresponding deterministic built-up structure model with average parameters, whose values are $\overline{\lambda_1} = 311.39\text{Hz}$, $\overline{\lambda_2} = 369.03\text{Hz}$, $\overline{\lambda_3} = 707.47\text{Hz}$, $\overline{\lambda_4} = 736.54\text{Hz}$, $\overline{\lambda_5} = 835.93\text{Hz}$,

$\overline{\lambda_6} = 889.67\text{Hz}$. While each random scatter denotes the eigenvalue of the corresponding random parameters with the given sample. It can be seen that the first two eigenvalues are well separated and little statistical overlap exists between them. However, the third to sixth eigenvalues are close to each other and there is distinct statistical overlap between them. Besides, the scatter degree becomes larger for higher modes than smaller modes, indicating that uncertainties in stiffness and mass distributions play a more important role for higher modes. The probability density distribution curves from the MSC results (using kernel density estimation) calculated by both the numerical perturbation method and WW algorithm are shown in Fig. 9(a) corresponds to the first two eigenvalues which are well separated, whereas Fig. 9(b) related to the third-sixth eigenvalues which are close. The results agree well with the scattering pattern of stochastic eigenvalues. Combined with Fig. 8 and Fig. 9, the distribution of stochastic eigenvalues can be considered in the following two forms:

Case 1: *Well separated eigenvalues.* As in Fig. 9(a), the first two eigenvalues are well separated. The first two deterministic eigenvalues of the corresponding baseline model are given by

$$\overline{\lambda_1} = 311.39\text{Hz} \quad \text{and} \quad \overline{\lambda_2} = 369.03\text{Hz} \tag{46}$$

It can be seen that there is little statistical overlap between them because the eigenvalues are well separated.

Case 2: *Close eigenvalues.* As in Fig. 9(b), the third to fourth and fifth to sixth eigenvalues are close to each other. As shown in Fig. 8, the deterministic eigenvalues of the last four eigenvalues are

$$\overline{\lambda_3} = 707.47\text{Hz}, \quad \overline{\lambda_4} = 736.54\text{Hz}, \quad \overline{\lambda_5} = 835.93\text{Hz} \quad \text{and} \quad \overline{\lambda_6} = 889.67\text{Hz} \tag{47}$$
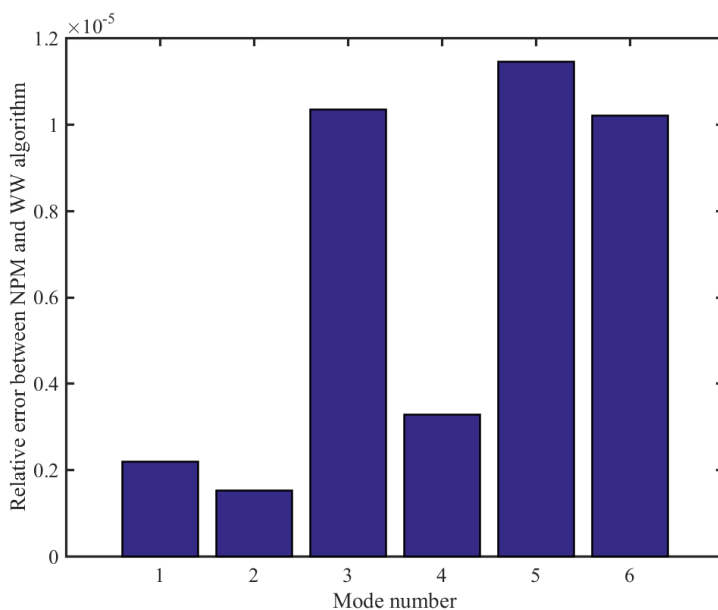

Fig. 10: Relative error of the mean of the first six stochastic eigenvalues of the beam built-up structures shown in Fig. 2 based on random variable model calculated by numerical perturbation method(NPM) and Wittrick-Williams(WW) algorithm(Benchmark method).

Clearly $\overline{\lambda_3}$ and $\overline{\lambda_4}$ are close to each other, while $\overline{\lambda_5}$ and $\overline{\lambda_6}$ are close to each other. There is significant statistical overlap between the third to fourth and fifth to sixth eigenvalues which can also be verified from Fig. 9.

Fig. 10 shows the relative error of the mean of the first six stochastic natural frequencies of 1500 samples by using numerical perturbation method compared to those by the WW algorithm. These errors are very small(less than 1.2×10^{-5}) considering that the strength of randomness for all random variables ($EA(\theta)$, $EI(\theta)$ and $m(\theta)$) are 10%. The well separated first two eigenvalues have a relatively small error, whereas the errors corresponding to third, fourth, fifth and sixth stochastic natural frequencies are relatively higher. This is expected since normally close eigenvalues introduce relatively more challenge to eigenvalue solution techniques than well-separated eigenvalues.

Table 3: The mean of natural frequencies covering low-, mid- to high-frequencies ranges for the beam built-up structure shown in Fig. 2 based on random variable model, computed by both the Wittrick-Williams(WW) algorithm and the numerical perturbation method(NPM), compared with the corresponding eigenvalues of deterministic model computed from the WW algorithm.

Modes	Deterministic model	Random variable modal	
	WW algorithm(Hz)	WW algorithm(Hz)	NPM(Hz)
1	311.39	310.95	310.95
2	369.03	369.17	369.17
3	707.47	702.07	702.08
30	3849.2	3843.6	3843.8
40	5358.0	5355.5	5355.6
50	6829.2	6890.6	6890.4
100	16324	16226	16226
Computation times(s)		174.05	120.19

In order to demonstrate the reliability and efficiency of the proposed NPM, Table 3 shows the mean of natural frequencies covering low-, mid- to high-frequencies ranges for the beam built-up structure computed by both the Wittrick-Williams(WW) algorithm and the numerical perturbation method(NPM) based on random variable model, and compared with the corresponding eigenvalues of deterministic model computed from the WW algorithm. It can be seen that the mean results calculated by the proposed NPM matches very well to those by the benchmark solutions computed by the Wittrick-Williams(WW) algorithm within the whole frequencies ranges. Moreover, the proposed NPM requires only three quarters of the computation time of the WW algorithm. The mean and the absolute value of standard deviation of the first 100 stochastic natural frequencies of 1500 samples calculated by the two methods are shown in Figs. 11(a) and (b) respectively. It can be seen that both the curves follow each other very closely. Fig. 12 shows the mean(a) and standard deviation(b) of the first three stochastic mode shapes of the beam built-up structures based on random variables model by using both Wittrick-Williams(WW) algorithm and numerical perturbation method(NPM). All mode shapes are normalized for maximum displacement. It can be seen that the mean of the first three stochastic mode shapes obtained by the two methods are very consistent.
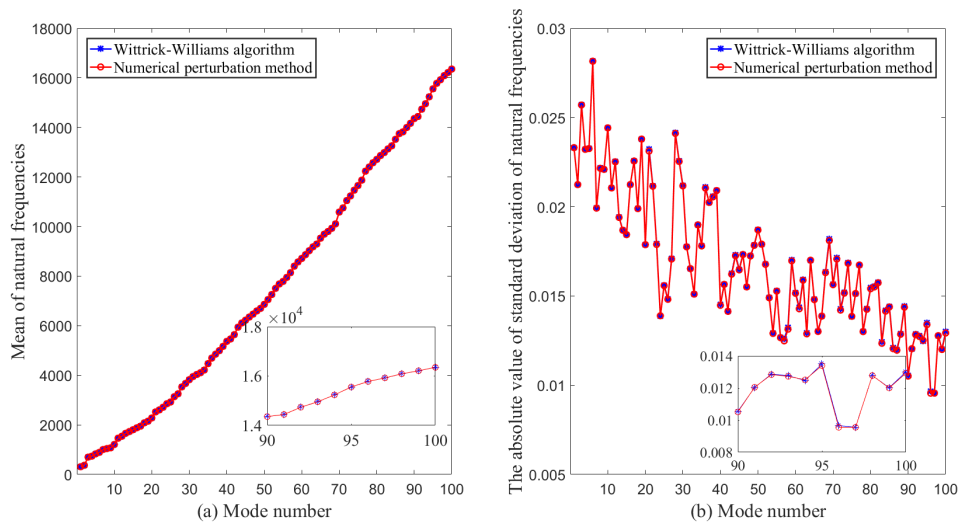
Fig. 11: The statistics of the first 100 natural frequencies of the beam built-up structures shown in Fig.2 based on random variable models by using the numerical perturbation method(NPM) and Wittrick-Williams(WW) algorithm. (a) Mean and (b) The absolute value of standard deviation of the first 100 stochastic natural frequencies.

(a) Mode 1   (a) Mode 2   (a) Mode 3

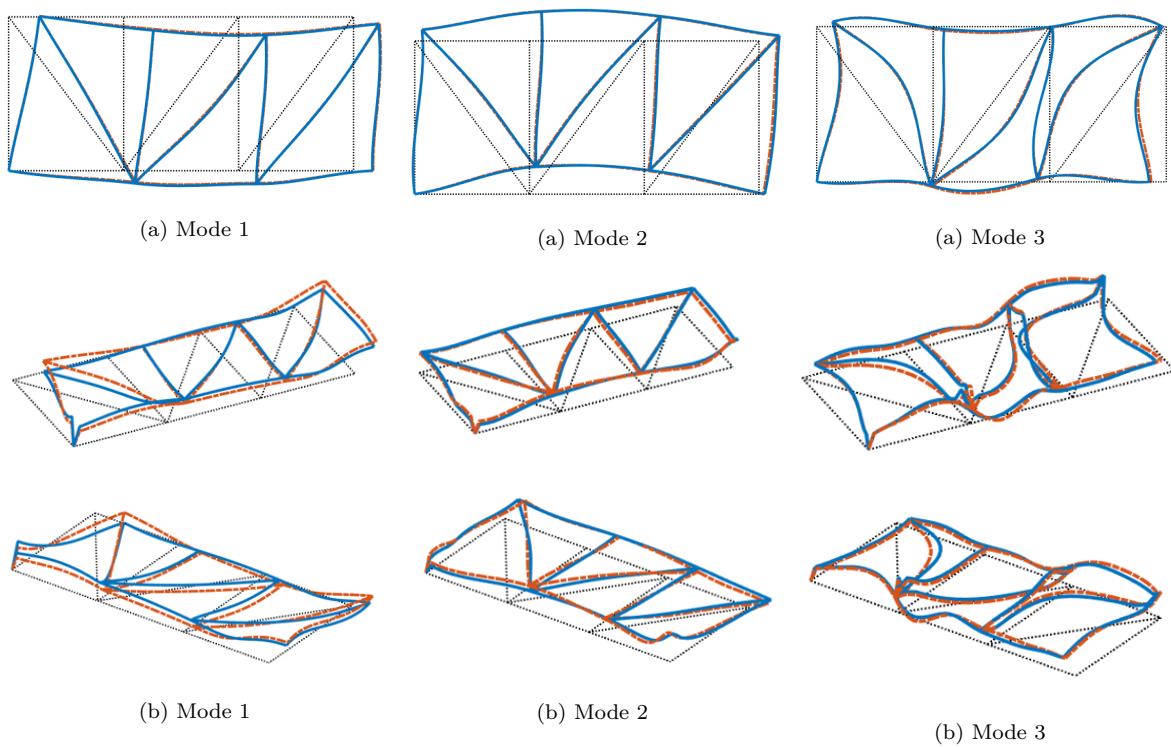(b) Mode 1   (b) Mode 2   (b) Mode 3

Fig. 12: The statistics of the first three mode shapes of the beam built-up structures shown in Fig.2 based on random variable models by using the numerical perturbation method(NPM) and Wittrick-Williams(WW) algorithm. (a) Mean and (b) standard deviation of the first three stochastic mode shapes. '――' Numerical perturbation method, '――' Wittrick-Williams algorithm.

4.2. Modal analysis of the random field model

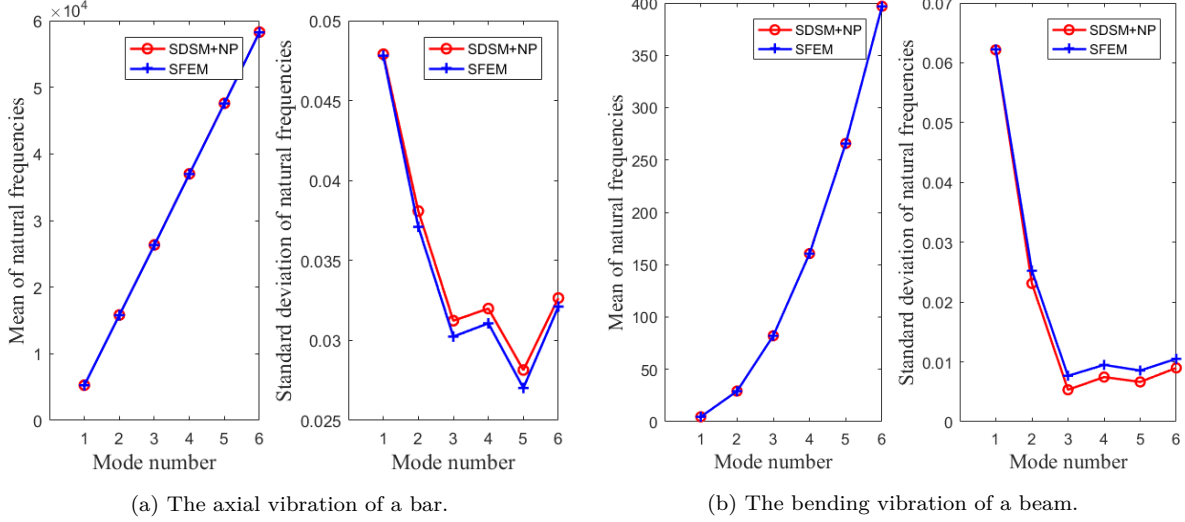(a) The axial vibration of a bar. (b) The bending vibration of a beam.

Fig. 13: The statistics of the first six natural frequencies of the axial vibration and the bending vibration of a beam based on random field models by using the SDSM combined with the numerical perturbation method(SDSM+NP) and SFEM. (a) Mean and (b) standard deviation of the first six stochastic natural frequencies.

First, two simple numerical examples are considered to illustrate the application of the method proposed in this paper for axial vibration and bending vibration of a clamp-free beam respectively. The mean material properties of the beam are considered as $\rho_0 = 7800\text{kg/m}^3$ and $E_0 = 210\text{GPa}$. The length of the beam is $L = 1.5\text{m}$ and the rectangular cross section has width 40.06mm and thickness 2.05mm. The area moment of inertia of the cross-section $I_0 = 2.876 \times 10^{-11}\text{m}^4$. The 'strength parameters' ϵ is assumed to be 0.1, that is, $\epsilon_{EI} = 0.1$, $\epsilon_m = 0.1$ and $\epsilon_{AE} = 0.1$. The correlation length of the random fields describing $EI(x)$, $m(x)$ and AE are assumed to be $L/2$.

The mean and the standard deviation of the first six stochastic natural frequencies of 1500 samples of axial vibration and bending vibration of a beam obtained by using the SDSM combined with the numerical perturbation method(NPM) are shown in Fig. 13, compared with the SFEM results. It can be seen that the results obtained from the SFEM match those of the SDSM developed in this paper with excellent accuracy. In addition, it can be found that for the same standard deviation, the discrete degree of natural frequencies of the axial vibration of a beam is significantly affected by the random field model. Table 4 shows the mean of natural frequencies covering low-, mid- to high-frequencies ranges for the axial vibration and the bending vibration of a beam, computed by both the SDSM combine with numerical perturbation method(SDSM+NPM) and SFEM. The results in the table have converged to four significant numbers. It can be seen from the table that with the increase of the number of elements, the convergence of low-order average eigenvalue of finite element calculation of random samples is relatively stable, while the convergence of high-order average eigenvalue is not stable. Moreover the method proposed in this paper has nearly four times the computational advantage compared with the stochastic finite element method(SFEM).

Table 4: The mean of natural frequencies covering low-, mid- to high-frequencies ranges for the axial vibration and the bending vibration of a beam based on random field models, computed by both the SDSM combine with numerical perturbation method(SDSM+NPM) and SFEM.

|	Method	Element number	Natural frequencies (Hz)						Computation times(s)
			1	2	3	30	50	100	
Axial vibration	SDSM (NPM)	1	5292.1	15876	26460	312233	523916	1053125	20.07
	SFEM (Eigs)	300	5292.1	15876	26467	312612	524595	1053824	32.16
		500	5292.1	15876	26463	312272	524002	1053298	57.02
		600	5292.1	15876	26460	312235	523918	1053145	119.72
Bending vibration	SDSM (NPM)	1	4.6915	29.229	82.389	11439	32208	130135	115.67
	SFEM (Eigs)	400	4.6919	29.257	82.730	11435	32212	130333	139.65
		500	4.6917	29.226	82.399	11440	32208	130165	250.65
		600	4.6913	29.229	82.385	11439	32208	130144	531.45
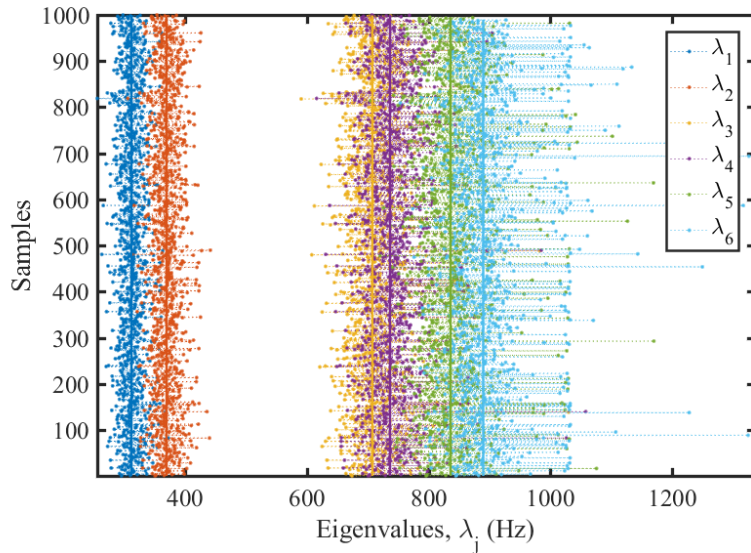
Fig. 14: Statistical scatter of the first six eigenvalues of the beam built-up structures shown in Fig. 2 based on random field model by using numerical perturbation method(NPM). The six vertical continuous lines represent the deterministic eigenvalues for the first six eigenmodes.

Another numerical example is the beam built-up structures shown in Fig. 2. The results for this example are obtained based on random field model by using numerical perturbation method(NPM) with 1500 samples. The random 'scatter' of the first six eigenvalues is shown in Fig. 14. The six vertical continuous lines represent the deterministic eigenvalues for the corresponding built-up structure model with average parameters, whose values are $\overline{\lambda_1} = 311.39\text{Hz}$, $\overline{\lambda_2} = 369.03\text{Hz}$, $\overline{\lambda_3} = 707.47\text{Hz}$, $\overline{\lambda_4} = 736.54\text{Hz}$, $\overline{\lambda_5} = 835.93\text{Hz}$, $\overline{\lambda_6} = 889.67\text{Hz}$. While each random scatter denotes the eigenvalue of the corresponding random filed with the given sample. It can be seen that compared with the eigenvalue results calculated by the random parameter model, the statistical overlap area of the first two orders of random eigenvalues corresponding to the random field model increases, but it still maintains a certain separation.And the statistical overlap region of the last four order eigenvalues also increases relatively. Besides, the scatter degree becomes larger for higher modes than smaller modes, indicating that uncertainties in stiffness and mass distributions play a more important role for higher modes.
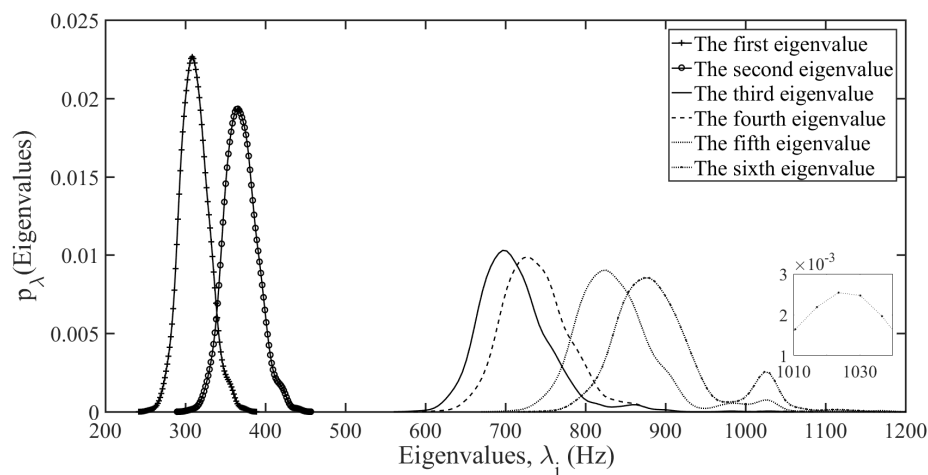

Fig. 15: Probability density functions of the first six stochastic natural frequencies of the beam built-up structures shown in Fig. 2 based on random fields model by using numerical perturbation method(NPM).

The probability density distribution curves from the MSC results (using kernel density estimation) calculated by numerical perturbation method(NPM) are shown in Fig. 15 which are corresponding to the first two eigenvalues and the last four eigenvalues of the scatter graph. There is a significant region of statistical overlap which can also be verified from the plot of the actual samples in Fig. 14. In addition, it is worth noting that in Fig. 15, although the probability density distribution we obtained is about the third to sixth determined eigenvalue solution, we can see that there is a probability distribution near the position of $\omega = 1020\text{Hz}$. This can be proved by the scattered point distribution at the same position in Fig. 14. This is similar to the seventh eigenvalue $\omega_7 = 1016.03\text{Hz}$ of the beam built-up structures. This is a very interesting phenomenon that first appeared in the eigenvalue probability density distribution curves of structural uncertain parameters. This is because after the introduction of stochastic dynamic stiffness theory, the core of the eigenvalue solution is the solution of J. The principle is described in Section 3.1. When J changes, $J+1$, the latter eigenvalue of the structure will be obtained. Here, when we are studying random problems, we set the dispersion of the sample to 0.1. Therefore,

the sample range in which the sixth eigenvalue will occur involves the frequency sample that will change J. The change will occur near the seventh eigenvalue, so that the given sample will be discrete near the seventh eigenvalue. This is why we can see the extra probability distribution in the probability density graph.

5. Conclusions

This paper proposes an efficient and reliable eigenvalue solution technique for free vibration analysis of beam-based built-up structures with parametric uncertainties. The method takes advantages of the stochastic dynamic stiffness (SDS) formulations that represent uncertain dynamic systems by using very few degrees of freedom. The dimension reduction has been achieved by combining the spectral discretization of the time-domain in the form of dynamic stiffness and the spectral discretization of the random domain in the form of Karhunen-Loève expansion. The numerical perturbation method based on the inverse iteration is proposed to extract the stochastic eigenvectors and eigenvalues from the stochastic dynamic stiffness formulations. The novelty of the proposed approach include:

- The accurate eigenvalues and eigenvectors are used as the initial iterative solutions of the numerical perturbation method to ensure the accuracy of the results.

- The numerical perturbation method is based on the inverse iteration method and uses the homotopy method to iterate the initial solution to obtain the stochastic eigenvalues and eigenvectors which has high robustness.

- In the iteration process, the calculation steps of each iteration are simple, which greatly improves the calculation efficiency. It is also well proved by comparing the results with other methods.

For the beam-based built-up structures, unlike the conventional finite element approach, a fine meshing is not necessary. This greatly saves the calculation time, particularly for stochastic problems. The advantages will be more obvious during the structure optimization design. In summary, the key advantages of the method developed are:

- It has obvious computational advantages for the modal analysis of medium and high-frequency vibration of beam built-up structures considering parameter uncertainties.

- This method can solve the dynamic stiffness formula of the arbitrarily assembled beam built-up structure and can conduct the stochastic modal analysis of the arbitrarily assembled beam built-up structure to study its dynamic characteristics.

- This method is applicable to the stochastic dynamic stiffness formulations based on both the random variable model and random field model. It can reasonably quantify the uncertainty of the structural parameters for different engineering cases, and propagate it into the structure to reflect the real properties of the structure.

By comparing with the WW algorithm and SFEM method, the accuracy and efficiency of the proposed method are verified. In the following research, the method will be used to further study plate structures and beam-plate built-up structures considering parameter uncertainties and connection uncertainties.

References

[1] D. V. Bambill, D. H. Felix, C. A. Rossit, Natural frequencies of thin, rectangular plates with holes or orthotropic "patches" carrying an elastically mounted mass, International Journal of Solids and Structures 43 (14-15) (2006) 4116–4135. doi:10.1016/j.ijsolstr.2005.03.051.

[2] M. U. Jen, E. B. Magrab, Natural frequencies and mode shapes of beams carrying a two degree of freedom spring-Mass system, Journal of Vibration and Acoustics, Transactions of the ASME 115 (2) (1993) 202–209. doi:10.1115/1.2930331.

[3] S. Adhikari, Joint statistics of natural frequencies of stochastic dynamic systems, Computational Mechanics 40 (4) (2007) 739–752.

[4] W. Ma, S. Xie, Z. Li, Mechanical performance of bio-inspired corrugated tubes with varying vertex configurations, International Journal of Mechanical Sciences 172 (November 2019) (2020) 105399. doi:10.1016/j.ijmecsci.2019.105399.

[5] S. Xie, H. Wang, C. Yang, H. Zhou, Z. Feng, Mechanical properties of combined structures of stacked multilayer Nomex® honeycombs (2020). doi:10.1016/j.tws.2020.106729.

[6] T. T. Soong, J. L. Bogdanoff, On the natural frequencies of a disordered linear chain of N degrees of freedom, International Journal of Mechanical Sciences 5 (3) (1963) 237–265. doi:10.1016/0020-7403(63)90052-3.

[7] J. V. Scheidt, W. Purkert, Random Eigenvalue Problems, North Holland, New York, 1983.

[8] Erik Vanmarcke, Random Fields Analysis and synthesis, 1984. doi:10.7551/mitpress/9780262013178.003.0014.

[9] S. Adhikari, C. S. Manohar, Dynamic analysis of framed structures with statistical uncertainties, International Journal for Numerical Methods in Engineering 44 (8) (1999) 1157–1178. doi:10.1002/(SICI)1097-0207(19990320)44:8<1157::AID-NME549>3.0.CO;2-5.

[10] Stefanou G, Stochastic Finite Elements: A Spectral Approach, Computer Methods in Applied Mechanics and Engineering 198 (9) (2009) 1031–1051.

[11] R. G. Ghanem, R. M. Kruger, Numerical solution of spectral stochastic finite element systems, Computer Methods in Applied Mechanics and Engineering 129 (3) (1996) 289–303. doi:10.1016/0045-7825(95)00909-4.

[12] G. Stefanou, The stochastic finite element method: Past, present and future, Computer Methods in Applied Mechanics and Engineering 198 (9-12) (2009) 1031–1051. doi:10.1016/j.cma.2008.11.007.

[13] M. Xu, J. Du, C. Wang, Y. Li, L. Wang, J. Chen, A dual-layer dimension-wise fuzzy finite element method for structural analysis with epistemic uncertainties, Fuzzy Sets and Systems 367 (2019) 68–81. doi:10.1016/j.fss.2018.08.010.

[14] M. Xu, J. Du, C. Wang, Y. Li, J. Chen, A dual-layer dimension-wise fuzzy finite element method (DwFFEM) for the structural-acoustic analysis with epistemic uncertainties, Mechanical Systems and Signal Processing 128 (2019) 617–635. doi:10.1016/j.ymssp.2019.04.006.

[15] B. E. Vanmarcke, M. Asce, M. Grigoriu, Stochastic finite element analysis of simple beams, Journal of Engineering Mechanics 109 (5) (1984) 1203–1214.

[16] T. Hisada, S. Nakagiri, Stochastic finite element method developed for structural safety and reliability, Elsevier Sci Publ Co (Dev in Civ Eng, 4), 1981, pp. 395–408.

[17] M. Shinozuka, Structural response variability, Journal of Engineering Mechanics, ASCE 113 (6) (1987) 825–842.

[18] W. D. Iwan, H. Jensen, On the dynamic response of continuous systems including model uncertainty, Journal of Applied Mechanics, Transactions ASME 60 (2) (1993) 484–490. doi:10.1115/1.2900819.

[19] C. C. Li, A. Kiureghian, Optimal discretization of random fields, Journal of Engineering Mechanics 119 (6) (1993) 1136–1154.

[20] W. K. Liu, T. Belytschko, A. Mani, Random field finite elements, International Journal for Numerical Methods in Engineering 23 (1986) 1831–1845.

[21] George Deodatis, Weighted integral method. I: Stochastic stiffness matrix, Journal of Engineering Mechanics, ASCE 117 (8) (1992) 1851–1864.

[22] S. Adhikari, M. I. Friswell, Random matrix eigenvalue problems in structural dynamics, International Journal for Numerical Methods in Engineering 69 (3) (2007) 562–591.

[23] R. A. Ibrahim, Structural dynamics with parameter uncertainties, Applied Mechanics Reviews, ASME 40 (3) (1987) 309–328.

[24] H. Benaroya, Random eigenvalues, algebraic methods and structural dynamic models, Applied Mathematics and Computation 52 (1992) 37–66.

[25] C. S. Manohar, R. A. Ibrahim, Progress in structural dynamics with stochastic parameter variations: 1987 to 1998, Applied Mechanics Reviews, ASME 52 (5) (1999) 177–197.

[26] J. Wu, Z. Luo, H. Li, N. Zhang, A new hybrid uncertainty optimization method for structures using orthogonal series expansion, Applied Mathematical Modelling 45 (2017) 474–490. doi:10.1016/j.apm.2017.01.006.

[27] J. Wu, Z. Luo, N. Zhang, Y. Zhang, P. D. Walker, Uncertain dynamic analysis for rigid-flexible mechanisms with random geometry and material properties, Mechanical Systems and Signal Processing 85 (2017) 487–511. doi:10.1016/j.ymssp.2016.08.040.

[28] D. K. Wilson, C. L. Pettit, V. E. Ostashev, S. N. Vecherin, Description and quantification of uncertainty in outdoor sound propagation calculations, The Journal of the Acoustical Society of America 136 (3) (2014) 1013–1028. doi:10.1121/1.4890644.

[29] K. Sarkar, R. Ganguli, D. Ghosh, I. Elishakoff, Random eigenvalue characterization for free vibration of axially loaded Euler-Bernoulli beams, AIAA Journal 56 (9) (2018) 3757–3765. doi:10.2514/1.J056942.

[30] M. Nurtaj Hossain, D. Ghosh, Adaptive reduced order modeling for nonlinear dynamical systems through a new a posteriori error estimator: Application to uncertainty quantification, International Journal for Numerical Methods in Engineering 121 (15) (2020) 3417–3441. doi:10.1002/nme.6365.

[31] M. Ghommem, M. R. Hajj, C. L. Pettit, P. S. Beran, Stochastic modeling of incident gust effects on aerodynamic lift, Journal of Aircraft 47 (5) (2010) 1720–1727. doi:10.2514/1.C000257.

[32] D. Ghosh, R. G. Ghanem, J. Red-Horse, Analysis of eigenvalues and modal interaction of stochastic systems, AIAA Journal 43 (10) (2005) 2196–2201.

[33] S. Adhikari, Complex modes in stochastic systems, Advances in Vibration Engineering 3 (1) (2004) 1–11.

[34] B. Pascual, S. Adhikari, Hybrid perturbation-polynomial chaos approaches to the random algebraic eigenvalue problem, Computer Methods in Applied Mechanics and Engineering 217-220 (1) (2012) 153–167.

[35] C. V. Verhoosel, M. A. Gutiérrez, S. J. Hulshoff, Iterative solution of the random eigenvalue problem with application to spectral stochastic finite element systems, International Journal for Numerical Methods in Engineering 68 (4) (2006) 401–424.

[36] S. Adhikari, Random eigenvalue problems revisited, Sādhanā - Proceedings of the Indian Academy of Engineering Sciences 31 (4) (2006) 293–314, (Special Issue on Probabilistic Structural Dynamics and Earthquake Engineering).

[37] J. R. Banerjee, F. W. Williams, Exact Bernoulli–Euler dynamic stiffness matrix for a range of tapered beams, International Journal for Numerical Methods in Engineering 21 (12) (1985) 2289–2302. doi:10.1002/nme.1620211212.

[38] J. R. Banerjee, Dynamic stiffness formulation for structural elements: A general approach, Computers and Structures 63 (1) (1997) 101–103. doi:10.1016/S0045-7949(96)00326-4.

[39] J. R. Banerjee, Dynamic stiffness formulation and its application for a combined beam and a two degree-of-freedom system, Journal of Vibration and Acoustics, Transactions of the ASME 125 (3) (2003) 351–358. doi:10.1115/1.1569943.

[40] C. S. Manohar, S. Adhikari, Dynamic stiffness of randomly parametered beams, Probabilistic Engineering Mechanics 13 (1) (1998) 39–51. doi:10.1016/s0266-8920(97)00006-4.

[41] X. Liu, X. Zhao, S. Adhikari, X. Liu, Stochastic dynamic stiffness for damped taut membranes, Computers & Structures 00 (2021) 1–29. doi:10.1016/j.compstruc.2021.106483.

[42] S. Adhikari, Doubly spectral stochastic finite-element method for linear structural dynamics, Journal of Aerospace Engineering 24 (3) (2011) 264–276. doi:10.1061/(ASCE)AS.1943-5525.0000070.

[43] N. C. Nigam, Introduction to Random Vibration, The MIT Press, Cambridge, Massachusetts, 1983.

[44] W. Wittrick, F. Williams, A general algorithm for computing natural conditions conditions of elastic structures, The Quarterly Journal of Mechanics and Applied Mathematics 24 (3) (1971) 263–284.

[45] J. R. Banerjee, F. W. Williams, Further flexural vibration curves for axially loaded beams with linear or parabolic taper, Journal of sound and vibration 102 (3) (1985) 315–327. doi:10.1016/S0022-460X(85)80145-0.

[46] H. Su, J. R. Banerjee, C. W. Cheung, Dynamic stiffness formulation and free vibration analysis of functionally graded beams, Composite Structures 106 (2013) 854–862. doi:10.1016/j.compstruct.2013.06.029.

[47] J. R. Banerjee, A. Ananthapuvirajah, Free vibration of functionally graded beams and frameworks using the dynamic stiffness method, Journal of Sound and Vibration 422 (2018) 34–47. doi:10.1016/j.jsv.2018.02.010.

[48] J. R. Banerjee, H. Su, D. R. Jackson, Free vibration of rotating tapered beams using the dynamic stiffness method, Journal of sound and vibration 298 (4-5) (2006) 1034–1054. doi:10.1016/j.jsv.2006.06.040.

[49] J. R. Banerjee, Free vibration of centrifugally stiffened uniform and tapered beams using the dynamic stiffness method, Journal of Sound and Vibration 233 (5) (2000) 857–875. doi:10.1006/jsvi.1999.2855.

[50] S. Yuan, K. Ye, F. Williams, Second order mode-finding method in dynamic stiffness matrix methods, Journal of sound and vibration 269 (3-5) (2004) 689–708. doi:10.1016/S0022-460X(03)00126-3.

Appendix A. Expression of spectral elemental matrices associated with the KL expansion of a beam member under axial vibration

This appendix gives the derivation of the matrices $\widetilde{\mathbf{K}}_j^a(\omega)$ and $\widetilde{\mathbf{M}}_j^a(\omega)$ with the KL expansion for the axial vibration of a beam member.

$$\widetilde{\mathbf{K}}_j^a(\omega) = \int_0^L \frac{\epsilon_{AE} A E_0 \cos(\alpha_j(-L/2 + x))}{\sqrt{L/2 + \frac{\sin(\alpha_j L)}{2\alpha_j}}} \left\{ \frac{\partial \mathrm{s}(x,\omega)}{\partial x} \right\} \left\{ \frac{\partial \mathrm{s}(x,\omega)}{\partial x} \right\}^T \mathrm{d}x \tag{A.1}$$

$$= \frac{\epsilon_{AE} A E_0}{\sqrt{(L/2 + c_\alpha s_\alpha/\alpha_j)}} \frac{a^2}{\alpha_j \left(4a^2 - \alpha_j^2\right)} \times$$

$$\begin{bmatrix} 2\alpha_j a c_{\alpha_j} cs + \left(-\alpha_j^2 + 4a^2 - \alpha_j^2 c^2\right) s_{\alpha_j} & \left(-2\alpha_j a + 2\alpha_j a c^2\right) c_{\alpha_j} + \alpha_j^2 s_{\alpha_j} cs \\ \left(-2\alpha_j a + 2\alpha_j a c^2\right) c_{\alpha_j} + \alpha_j^2 s_{\alpha_j} cs & -2\alpha_j a c_{\alpha_j} cs + \left(4a^2 - \alpha_j^2 + \alpha_j^2 c^2\right) s_{\alpha_j} \end{bmatrix} \tag{A.2}$$

In the above expression

$$c_{\alpha_j} = \cos\left(\alpha_j L/2\right) \quad \text{and} \quad s_{\alpha_j} = \sin\left(\alpha_j L/2\right) \tag{A.3}$$

and the eigenvalues α_j should be obtained by solving the transcendental Eq. (11) with $l = L/2$. In Eq. (A.1) the KL eigenfunction is shifted to take account of the fact that Eq. (11) is defined for $-L/2 \leq x \leq L/2$ while the element shape functions are defined over $0 \leq x \leq L$. In Eq. (A.1) we have used the identity $\sin(\alpha_j L) = 2\cos\left(\alpha_j L/2\right)\sin\left(\alpha_j L/2\right) = 2c_\alpha s_\alpha$. In a similar manner, using the expression of the eigenfunction for the even values

of j as in Eq. (12) one has

$$\widetilde{\mathbf{K}}_j^a(\omega) = \int_0^L \frac{\epsilon_{AE} A E_0 \sin(\alpha_j(-L/2+x))}{\sqrt{L/2 - \frac{\sin(\alpha_j L)}{2\alpha_j}}} \left\{ \frac{\partial \mathrm{s}(x,\omega)}{\partial x} \right\} \left\{ \frac{\partial \mathrm{s}(x,\omega)}{\partial x} \right\}^T \mathrm{d}x \qquad (A.4)$$

$$= \frac{\epsilon_{AE} A E_0}{\sqrt{(L/2 - c_\alpha s_\alpha/\alpha_j)}\, \alpha_j \left(4a^2 - \alpha_j^2\right)} \frac{a^2}{\times}$$
$$\begin{bmatrix} (-\alpha_j^2 + \alpha_j^2 c^2)\, c_{\alpha_j} + 2\alpha_j a s_{\alpha_j} cs & -\alpha_j^2 c_{\alpha_j} cs + 2\alpha_j a s_{\alpha_j} c^2 \\ -\alpha_j^2 c_{\alpha_j} cs + 2\alpha_j a s_{\alpha_j} c^2 & (\alpha_j^2 - \alpha_j^2 c^2)\, c_{\alpha_j} - 2\alpha_j a s_{\alpha_j} cs \end{bmatrix} \qquad (A.5)$$

The mass matrix can also be represented as Eqs. (14)-(17). The eigenvalues and eigenfunctions corresponding to the random field $H_m(x,\theta)$ needs to be used to obtain the elements of $\widetilde{\mathbf{M}}_j^a(\omega)$. Using the expression of the eigenfunction for the odd values of j as in Eq. (11) one has

$$\widetilde{\mathbf{M}}_j^a(\omega) = \int_0^L \frac{\epsilon_m m_0 \cos(\alpha_j(-L/2+x))}{\sqrt{L/2 + \frac{\sin(\alpha_j L)}{2\alpha_j}}} \mathrm{s}(x,\omega)\mathrm{s}^T(x,\omega)\, \mathrm{d}x \qquad (A.6)$$

$$= \frac{\epsilon_m m_0}{\sqrt{(L/2 + c_\alpha s_\alpha/\alpha_j)}\, \alpha_j \left(4a^2 - \alpha_j^2\right)} \frac{1}{\times}$$
$$\begin{bmatrix} -2\alpha_j a c_{\alpha_j} cs + (4a^2 - \alpha_j^2 + \alpha_j^2 c^2)\, s_{\alpha_j} & (2\alpha_j a - 2\alpha_j a c^2)\, c_{\alpha_j} - \alpha_j^2 s_{\alpha_j} cs \\ (2\alpha_j a - 2\alpha_j a c^2)\, c_{\alpha_j} - \alpha_j^2 s_{\alpha_j} cs & 2\alpha_j a c_{\alpha_j} cs + (-\alpha_j^2 + 4a^2 - \alpha_j^2 c^2)\, s_{\alpha_j} \end{bmatrix} \qquad (A.7)$$

In the above expression the eigenvalues α_j should be obtained by solving the transcendental Eq. (11). In a similar manner, using the expression of the eigenfunction for the even values of j as in Eq. (12) one has

$$\widetilde{\mathbf{M}}_j^a(\omega) = \int_0^L \frac{\epsilon_m m_0 \sin(\alpha_j(-L/2+x))}{\sqrt{L/2 - \frac{\sin(\alpha_j L)}{2\alpha_j}}} \mathrm{s}(x,\omega)\mathrm{s}^T(x,\omega)\, \mathrm{d}x \qquad (A.8)$$

$$= \frac{\epsilon_m m_0}{\sqrt{(L/2 - c_\alpha s_\alpha/\alpha_j)}\, \alpha_j \left(4a^2 - \alpha_j^2\right)} \frac{1}{\times}$$
$$\begin{bmatrix} (\alpha_j^2 - \alpha_j^2 c^2)\, c_{\alpha_j} - 2\alpha_j a s_{\alpha_j} cs & \alpha_j^2 c_{\alpha_j} cs - 2\alpha_j a s_{\alpha_j} c^2 \\ \alpha_j^2 c_{\alpha_j} cs - 2\alpha_j a s_{\alpha_j} c^2 & (-\alpha_j^2 + \alpha_j^2 c^2)\, c_{\alpha_j} + 2\alpha_j a s_{\alpha_j} cs \end{bmatrix} \qquad (A.9)$$

Eqs. (A.1)–(A.8) completely define the random parts of the elemental stiffness and mass matrices. The exact closed-form expression of the elements of the above four matrices further reduces the computational cost in deriving these matrices.

Appendix B. Expression of spectral elemental matrices associated with the KL expansion of a beam member under bending vibration

This appendix gives the derivation of the matrices $\widetilde{\mathbf{K}}_0^b(\omega)$, $\widetilde{\mathbf{M}}_0^b(\omega)$, $\widetilde{\mathbf{K}}_j^b(\omega)$ and $\widetilde{\mathbf{M}}_j^b(\omega)$ and the explicit expressions for the spectral stiffness and mass matrices associated with the KL expansion for the bending vibration of a beam member. The deterministic stiffness

matrix and mass matrix can be obtained from Eq. (15), $\widetilde{\mathbf{K}}_0^b(\omega)$ and $\widetilde{\mathbf{M}}_0^b(\omega)$ are obtained by the following equation

$$\widetilde{\mathbf{K}}_0^b(\omega) = EI_0 \int_{x=0}^{L} \left\{ \frac{\partial^2 \mathrm{s}(x,\omega)}{\partial x^2} \right\} \left\{ \frac{\partial^2 \mathrm{s}(x,\omega)}{\partial x^2} \right\}^T \mathrm{d}x \tag{B.1}$$

$$= \frac{EI_0 b^3}{2} \begin{bmatrix} bL - cs & 1 - c^2 & cS - sC & -1 + cC - sS \\ 1 - c^2 & cs + bL & 1 - cC - sS & -cS - sC \\ cS - sC & 1 - cC - sS & CS - bL & -1 + C^2 \\ -1 + cC - sS & -cS - sC & -1 + C^2 & CS + bL \end{bmatrix} \tag{B.2}$$

$$\widetilde{\mathbf{M}}_0^b(\omega) = m_0 \int_{x=0}^{L} \mathrm{s}(x,\omega)\mathrm{s}^T(x,\omega)\mathrm{d}x \tag{B.3}$$

$$= \frac{m_0}{2b} \begin{bmatrix} bL - cs & 1 - c^2 & -cS + sC & 1 - cC + sS \\ 1 - c^2 & cs + bL & -1 + cC + sS & cS + sC \\ -cS + sC & -1 + cC + sS & CS - bL & -1 + C^2 \\ 1 - cC + sS & cS + sC & -1 + C^2 & CS + bL \end{bmatrix} \tag{B.4}$$

Note that for each j there will be two different matrices corresponding to the two eigenfunctions to obtain the matrices associated with the random components.

Using the expression of the eigenfunction for the odd values of j as in Eq. (11) one has

$$\widetilde{\mathbf{K}}_j^b(\omega) = \int_0^L \frac{\epsilon_{EI} EI_0 \cos[\alpha_j(-L/2 + x)]}{\sqrt{L/2 + \frac{\sin(\alpha_j L)}{2\alpha_j}}} \left\{ \frac{\partial^2 \mathrm{S}(x,\omega)}{\partial x^2} \right\} \left\{ \frac{\partial^2 \mathrm{S}(x,\omega)}{\partial x^2} \right\}^T dx$$
$$= \frac{\epsilon_{EI} EI_0}{\sqrt{(L/2 + c_\alpha s_\alpha/\alpha_j)}} \widehat{\mathbf{K}}_j \tag{B.5}$$

where c_α, s_α are defined in Eq. (A.3) and $\widehat{\mathbf{K}}_j \in \mathbb{C}^{4\times 4}$ is a symmetric matrix obtained in Appendix Appendix A. In a similar manner, using the expression of the eigenfunction for the even values of j as in Eq. (12) one has

$$\widetilde{\mathbf{K}}_j^b(\omega) = \int_0^L \frac{\epsilon_{EI} EI_0 \sin[\alpha_j(-L/2 + x)]}{\sqrt{L/2 - \frac{\sin(\alpha_j L)}{2\alpha_j}}} \left\{ \frac{\partial^2 \mathrm{S}(x,\omega)}{\partial x^2} \right\} \left\{ \frac{\partial^2 \mathrm{S}(x,\omega)}{\partial x^2} \right\}^T dx$$
$$= \frac{\epsilon_{EI} EI_0}{\sqrt{(L/2 - c_\alpha s_\alpha/\alpha_j)}} \widehat{\mathbf{K}}_j \tag{B.6}$$

The mass matrix can also be represented as above. The eigenvalues and eigenfunctions corresponding to the random field $H_m(x,\theta)$ needs to be used to obtain the elements of $\widetilde{\mathbf{M}}_j^b(\omega)$. Using the expression of the eigenfunction for the odd values of j as in Eq. (11) one has

$$\widetilde{\mathbf{M}}_j^b(\omega) = \int_0^L \frac{\epsilon_m m_0 \cos(\alpha_j(-L/2 + x))}{\sqrt{L/2 + \frac{\sin(\alpha_j L)}{2\alpha_j}}} \mathrm{s}(x,\omega)\mathrm{s}^T(x,\omega) \, \mathrm{d}x \tag{B.7}$$
$$= \frac{\epsilon_m m_0}{\sqrt{(L/2 + c_\alpha s_\alpha/\alpha_j)}} \widehat{\mathbf{M}}_j$$

In the above expression the eigenvalues α_j should be obtained by solving the transcendental Eq. (11). In a similar manner, using the expression of the eigenfunction for the even values of j as in Eq. (12) one has

$$\widetilde{\mathbf{M}}_j^b(\omega) = \int_0^L \frac{\epsilon_m m_0 \sin(\alpha_j(-L/2+x))}{\sqrt{L/2 - \frac{\sin(2\alpha_j a)}{2\alpha_j}}} \mathbf{s}(x,\omega)\mathbf{s}^T(x,\omega)\,\mathrm{d}x \tag{B.8}$$

$$= \frac{\epsilon_m m_0}{\sqrt{(L/2 - c_\alpha s_\alpha/\alpha_j)}}\widehat{\mathbf{M}}_j$$

Eqs. (B.5)-(B.8) completely define the random parts of the elemental stiffness and mass matrices. The definite integrals appearing in these expressions can be evaluated in closed-form. This further reduces the computational cost in deriving the elemental matrices. The exact closed-form expression of the elements of the above four matrices can be obtained as

$$\widehat{K}_{11} = \frac{4b^6 s_{\alpha_j} - 2b^5\alpha_j c_{\alpha_j}cs + \left(-\alpha_j{}^2+\alpha_j{}^2c^2\right)s_{\alpha_j}b^4}{-\alpha_j{}^3+4\alpha_j b^2}$$

$$\widehat{K}_{12} = \frac{\left(2-2c^2\right)c_{\alpha_j}b^5 - b^4\alpha_j s_{\alpha_j}cs}{-\alpha_j{}^2+4b^2}$$

$$\widehat{K}_{13} = \frac{(2cS-2sC)c_{\alpha_j}b^7+(2\alpha_j+2\alpha_j Cc)s_{\alpha_j}b^6+\left(-\alpha_j{}^2Cs-\alpha_j{}^2cS\right)c_{\alpha_j}b^5 - b^4\alpha_j{}^3 s_{\alpha_j}Ss}{4b^4+\alpha_j{}^4}$$

$$\widehat{K}_{14} = \frac{(-2Ss-2+2Cc)c_{\alpha_j}b^7+2b^6\alpha_j s_{\alpha_j}cS+\left(-\alpha_j{}^2Ss+\alpha_j{}^2-\alpha_j{}^2Cc\right)c_{\alpha_j}b^5 - b^4\alpha_j{}^3 Cs_{\alpha_j}s}{4b^4+\alpha_j{}^4}$$

$$\widehat{K}_{22} = \frac{4b^6 s_{\alpha_j} + 2b^5\alpha_j c_{\alpha_j}cs + \left(-\alpha_j{}^2-\alpha_j{}^2c^2\right)s_{\alpha_j}b^4}{-\alpha_j{}^3+4\alpha_j b^2}$$

$$\widehat{K}_{23} = \frac{(2-2Ss-2Cc)c_{\alpha_j}b^7-2b^6\alpha_j Cs_{\alpha_j}s+\left(-\alpha_j{}^2Cc+\alpha_j{}^2Ss+\alpha_j{}^2\right)c_{\alpha_j}b^5 - b^4\alpha_j{}^3 s_{\alpha_j}cS}{4b^4+\alpha_j{}^4}$$

$$\widehat{K}_{24} = \frac{(-2cS-2sC)c_{\alpha_j}b^7-2b^6\alpha_j s_{\alpha_j}Ss+\left(\alpha_j{}^2Cs-\alpha_j{}^2cS\right)c_{\alpha_j}b^5+\left(-\alpha_j{}^3-\alpha_j{}^3Cc\right)s_{\alpha_j}b^4}{4b^4+\alpha_j{}^4}$$

$$\widehat{K}_{33} = \frac{-4b^6 s_{\alpha_j} + 2b^5\alpha_j SCc_{\alpha_j} + \left(\alpha_j{}^2C^2-\alpha_j{}^2\right)s_{\alpha_j}b^4}{4\alpha_j b^2+\alpha_j{}^3}$$

$$\widehat{K}_{34} = \frac{\left(-2+2C^2\right)c_{\alpha_j}b^5+b^4\alpha_j SCs_{\alpha_j}}{4b^2+\alpha_j{}^2}$$

$$\widehat{K}_{44} = \frac{4b^6 s_{\alpha_j} + 2b^5\alpha_j SCc_{\alpha_j} + \left(\alpha_j{}^2C^2+\alpha_j{}^2\right)s_{\alpha_j}b^4}{4\alpha_j b^2+\alpha_j{}^3}.$$

The subscript j is omitted in $\widehat{K}$ for notational convenience. Because the matrix is symmetric, only the upper triangular part is shown. All the terms appearing in the above expressions have been defined in the main body of the chapter. The elements of the stiffness matrix associated with the even values of j in Eq. (B.6) can be obtained as

$$\widehat{K}_{11} = \frac{-2b^5 s_{\alpha_j}cs + \left(\alpha_j-\alpha_j c^2\right)c_{\alpha_j}b^4}{-\alpha_j{}^2+4b^2}$$

$$\widehat{K}_{12} = \frac{b^4 c\alpha_j c_{\alpha_j}s - 2b^5 c^2 s_{\alpha_j}}{-\alpha_j{}^2+4b^2}$$

$$\widehat{K}_{13} = \frac{(2cS-2sC)s_{\alpha_j}b^7+(-2\alpha_j Cc+2\alpha_j)c_{\alpha_j}b^6+\left(-\alpha_j{}^2Cs-\alpha_j{}^2cS\right)s_{\alpha_j}b^5+b^4\alpha_j{}^3 c_{\alpha_j}Ss}{4b^4+\alpha_j{}^4}$$

$$\widehat{K}_{14} = \frac{(2Cc-2Ss+2)s_{\alpha_j}b^7-2b^6\alpha_j c_{\alpha_j}cS+\left(-\alpha_j{}^2Cc-\alpha_j{}^2-\alpha_j{}^2Ss\right)s_{\alpha_j}b^5+b^4\alpha_j{}^3 Cc_{\alpha_j}s}{4b^4+\alpha_j{}^4}$$

$$\widehat{K}_{22} = \frac{\left(-2s_{\alpha_j}\alpha_j\cos(\alpha_j L)cs+2c_{\alpha_j}\alpha_j\sin(\alpha_j L)cs\right)b^5+\left(\left(-\alpha_j{}^2+\alpha_j{}^2\cos(\alpha_j L)c^2\right)c_{\alpha_j}+s_{\alpha_j}\alpha_j{}^2\sin(\alpha_j L)c^2\right)b^4}{-\alpha_j{}^3+4\alpha_j b^2}$$

$$\widehat{K}_{23} = \frac{(-2-2Cc-2Ss)s_{\alpha_j}b^7+2b^6\alpha_j Cc_{\alpha_j}s+\left(-\alpha_j{}^2Cc-\alpha_j{}^2+\alpha_j{}^2Ss\right)s_{\alpha_j}b^5+b^4\alpha_j{}^3 c_{\alpha_j}cS}{4b^4+\alpha_j{}^4}$$

$$\widehat{K}_{24} = \frac{(-2cS-2sC)s_{\alpha_j}b^7+2b^6\alpha_j c_{\alpha_j}Ss+\left(\alpha_j{}^2Cs-\alpha_j{}^2cS\right)s_{\alpha_j}b^5+\left(-\alpha_j{}^3+\alpha_j{}^3Cc\right)c_{\alpha_j}b^4}{4b^4+\alpha_j{}^4}$$

$$\widehat{K}_{33} = \frac{2b^5SCs_{\alpha_j}+\left(\alpha_j-\alpha_jC^2\right)c_{\alpha_j}b^4}{4b^2+\alpha_j{}^2}$$

$$\widehat{K}_{34} = \frac{2C^2b^5s_{\alpha_j}-Cb^4\alpha_jSc_{\alpha_j}}{4b^2+\alpha_j{}^2}$$

$$\widehat{K}_{44} = \frac{2b^5SCs_{\alpha_j}+\left(\alpha_j-\alpha_jC^2\right)c_{\alpha_j}b^4}{4b^2+\alpha_j{}^2}.$$

The elements of the mass matrix associated with the odd values of j in Eq. (B.7) can be obtained as

$$\widehat{M}_{11} = \frac{4b^2s_{\alpha_j}-2b\alpha_jc_{\alpha_j}cs+\left(-\alpha_j{}^2+\alpha_j{}^2c^2\right)s_{\alpha_j}}{-\alpha_j{}^3+4\alpha_jb^2}$$

$$\widehat{M}_{12} = \frac{\left(2-2c^2\right)c_{\alpha_j}b-\alpha_js_{\alpha_j}cs}{-\alpha_j{}^2+4b^2}$$

$$\widehat{M}_{13} = \frac{(2cS-2sC)c_{\alpha_j}b^3+(2\alpha_j+2\alpha_jCc)s_{\alpha_j}b^2+\left(-\alpha_j{}^2Cs-\alpha_j{}^2cS\right)c_{\alpha_j}b-\alpha_j{}^3s_{\alpha_j}Ss}{4b^4+\alpha_j{}^4}$$

$$\widehat{M}_{14} = \frac{(-2Ss-2+2Cc)c_{\alpha_j}b^3+2b^2\alpha_js_{\alpha_j}cS+\left(-\alpha_j{}^2Ss+\alpha_j{}^2-\alpha_j{}^2Cc\right)c_{\alpha_j}b-\alpha_j{}^3Cs_{\alpha_j}s}{4b^4+\alpha_j{}^4}$$

$$\widehat{M}_{22} = \frac{4b^2s_{\alpha_j}+2b\alpha_jc_{\alpha_j}cs+\left(-\alpha_j{}^2-\alpha_j{}^2c^2\right)s_{\alpha_j}b}{-\alpha_j{}^3+4\alpha_jb^2}$$

$$\widehat{M}_{23} = \frac{(2-2Ss-2Cc)c_{\alpha_j}b^3-2b^2\alpha_jCs_{\alpha_j}s+\left(-\alpha_j{}^2Cc+\alpha_j{}^2Ss+\alpha_j{}^2\right)c_{\alpha_j}b-\alpha_j{}^3s_{\alpha_j}cS}{4b^4+\alpha_j{}^4}$$

$$\widehat{M}_{24} = \frac{(-2cS-2sC)c_{\alpha_j}b^3-2b^2\alpha_js_{\alpha_j}Ss+\left(\alpha_j{}^2Cs-\alpha_j{}^2cS\right)c_{\alpha_j}b+\left(-\alpha_j{}^3-\alpha_j{}^3Cc\right)s_{\alpha_j}}{4b^4+\alpha_j{}^4}$$

$$\widehat{M}_{33} = \frac{-4b^2s_{\alpha_j}+2b\alpha_jSCc_{\alpha_j}+\left(\alpha_j{}^2C^2-\alpha_j{}^2\right)s_{\alpha_j}}{4\alpha_jb^2+\alpha_j{}^3}$$

$$\widehat{M}_{34} = \frac{\left(-2+2C^2\right)c_{\alpha_j}b+\alpha_jSCs_{\alpha_j}}{4b^2+\alpha_j{}^2}$$

$$\widehat{M}_{44} = \frac{4b^2s_{\alpha_j}+2b\alpha_jSCc_{\alpha_j}+\left(\alpha_j{}^2C^2+\alpha_j{}^2\right)s_{\alpha_j}}{4\alpha_jb^2+\alpha_j{}^3}.$$

The elements of the mass matrix associated with the even values of j in Eq. (B.8) can be obtained as

$$\widehat{M}_{11} = \frac{-2bs_{\alpha_j}cs+\left(\alpha_j-\alpha_jc^2\right)c_{\alpha_j}}{-\alpha_j{}^2+4b^2}$$

$$\widehat{M}_{12} = \frac{c\alpha_jc_{\alpha_j}s-2bc^2s_{\alpha_j}}{-\alpha_j{}^2+4b^2}$$

$$\widehat{M}_{13} = \frac{(2cS-2sC)s_{\alpha_j}b^3+(-2\alpha_jCc+2\alpha_j)c_{\alpha_j}b^2+\left(-\alpha_j{}^2Cs-\alpha_j{}^2cS\right)s_{\alpha_j}b+\alpha_j{}^3c_{\alpha_j}Ss}{4b^4+\alpha_j{}^4}$$

$$\widehat{M}_{14} = \frac{(2Cc-2Ss+2)s_{\alpha_j}b^3-2b^2\alpha_jc_{\alpha_j}cS+\left(-\alpha_j{}^2Cc-\alpha_j{}^2-\alpha_j{}^2Ss\right)s_{\alpha_j}b+\alpha_j{}^3Cc_{\alpha_j}s}{4b^4+\alpha_j{}^4}$$

$$\widehat{M}_{22} = \frac{\left(-2s_{\alpha_j}\alpha_j\cos(\alpha_jL)cs+2c_{\alpha_j}\alpha_j\sin(\alpha_jL)cs\right)b+\left(\left(-\alpha_j{}^2+\alpha_j{}^2\cos(\alpha_jL)c^2\right)c_{\alpha_j}+s_{\alpha_j}\alpha_j{}^2\sin(\alpha_jL)c^2\right)}{-\alpha_j{}^3+4\alpha_jb^2}$$

$$\widehat{M}_{23} = \frac{(-2-2Cc-2Ss)s_{\alpha_j}b^3+2b^2\alpha_jCc_{\alpha_j}s+\left(-\alpha_j{}^2Cc-\alpha_j{}^2+\alpha_j{}^2Ss\right)s_{\alpha_j}b+\alpha_j{}^3c_{\alpha_j}cS}{4b^4+\alpha_j{}^4}$$

$$\widehat{M}_{24} = \frac{(-2cS-2sC)s_{\alpha_j}b^3+2b^2\alpha_jc_{\alpha_j}Ss+\left(\alpha_j{}^2Cs-\alpha_j{}^2cS\right)s_{\alpha_j}b+\left(-\alpha_j{}^3+\alpha_j{}^3Cc\right)c_{\alpha_j}}{4b^4+\alpha_j{}^4}$$

$$\widehat{M}_{33} = \frac{2bSCs_{\alpha_j}+\left(\alpha_j-\alpha_jC^2\right)c_{\alpha_j}}{4b^2+\alpha_j{}^2}$$

$$\widehat{M}_{34} = \frac{2C^2bs_{\alpha_j}-C\alpha_jSc_{\alpha_j}}{4b^2+\alpha_j{}^2}$$

$$\widehat{M}_{44} = \frac{2bSCs_{\alpha_j}+\left(\alpha_j-\alpha_jC^2\right)c_{\alpha_j}}{4b^2+\alpha_j{}^2}.$$